Target article

Adaptive neural networks for control of movement trajectories invariant under speed and force rescaling

Daniel Bullock * and Stephen Grossberg **

Boston University, Boston, USA

Abstract

Bullock, D. and S. Grossberg, 1991. Adaptive neural networks for control of movement trajectories invariant under speed and force rescaling (Target article). Human Movement Science 10, 3–53.

This article describes two neural network modules that form part of an emerging theory of how adaptive control of goal-directed sensory-motor skills is achieved by humans and other animals. The Vector-Integration-To-Endpoint (VITE) model suggests how synchronous multi-joint trajectories are generated and performed at variable speeds. The Factorization-of-LEngth-and-TEnsion (FLETE) model suggests how outflow movement commands from a VITE model may be performed at variable force levels without a loss of positional accuracy. The invariance of positional control under speed and force rescaling sheds new light upon a familiar strategy of motor skill development: skill learning begins with performance at low speed and low limb compliance and proceeds to higher speeds and compliances. The VITE model helps to explain many neural and behavioral data about trajectory formation, including data about neural coding within the posterior parietal cortex, motor cortex, and globus pallidus, and behavioral properties such as Woodworth's Law, Fitts' Law, peak acceleration as a function of movement amplitude and duration, isotonic arm movement properties before and after arm-deafferentation, central error correction properties of isometric contractions, motor priming without overt action, velocity amplification during target switching, velocity profile invariance across different movement distances, changes in velocity profile asymmetry across different movement durations, staggered onset times for controlling linear trajectories with synchronous offset times, changes in the ratio of maximum to average velocity during discrete versus serial movements, and shared properties of

arm and speech articulator movements. The FLETE model provides new insights into how spino-muscular circuits process variable forces without a loss of positional control. These results explicate the size principle of motor neuron recruitment, descending co-contractive compliance signals, Renshaw cells, Ia interneurons, fast automatic reactive control by ascending feedback from muscle spindles, slow adaptive predictive control via cerebellar learning using muscle spindle error signals to train adaptive movement gains, fractured somatotopy in the opponent organization of cerebellar learning, adaptive compensation for variable moment-arms, and force feedback from Golgi tendon organs. More generally, the models provide a computational rationale for the use of nonspecific control signals in volitional control, or 'acts of will', and of efference copies and opponent processing in both reactive and adaptive motor control tasks.

1. Position-code invariance and skill development

In natural motor control, an organism frequently controls two or more motor system variables simultaneously. For example, in reaching to a target, an organism can control both the speed and the form, which includes direction and endpoint, of the reaching movement; and once a new posture is assumed, the organism can continuously vary the compliance of its joints without inadvertently changing joint angle. Despite wide fluctuations in the muscular energy expended, the positions attained to perform movement at variable speeds or to hold a posture at variable compliances are remarkably invariant. We often call this fundamental property *position-code invariance*.

Whenever an invariance is observed in the behavior of a complex system, questions arise regarding the mechanisms by which it is achieved. By definition, a complex system is composed of partially independent subsystems, whose interactions give rise to the complex system's competence. However, whenever two subsystems are connected there is no guarantee that prior system competence will be preserved. This theme has been recognized by many movement control researchers (e.g. Bernstein 1967). The point was also recognized by Piaget as a postulate in his theory of cognitive equilibration: 'Modifying a scheme must destroy neither its closure as a cycle of interdependent processes nor its previous powers of assimilation' (Piaget 1985: 6).

The same issue has emerged as a central theme within neural network theories of cognition and behavior (e.g. Grossberg 1978, 1982; Grossberg and Kuperstein 1986, 1989). The particular genus of 'preservation under interaction', or invariance problem, treated in this article has been called the *pattern-energy factorization* problem (Grossberg 1970, 1973, 1982) to emphasize that many neural networks are

designed to factor pattern differences from overall activity levels. The overall activity level may be controlled by a nonspecific signal broadcast to all network sites. A nonspecific signal is a scalar signal that is generated at a single command source and delivered, through a parallel fan-out of pathways, to many target cells. Using a nonspecific signal is one device whereby voluntary control of speed or compliance may be simplified. For this control strategy to work, the target cells must be designed to react in an appropriate state-dependent manner. Then a single nonspecific signal can be used to effect conscious control over a large array of cells without the need for conscious control of each cell in the array.

The pattern-energy factorization problem needs careful analysis because all biological neurons exhibit electrical potentials and currents which fluctuate within a bounded range. Thus broadcasting the same nonspecific signal to an entire array of cells could raise the baseline level of activity across the array and push the activities of many cells toward their maximum potentials. The nonspecific signal could thereby homogenize, or compress, the spatial pattern of cell activities originally induced by specific inputs to the same array. Because information in a neural network is carried by such spatial patterns, a nonspecific signal could easily become information destroying. In what follows, we show how to design neural control circuits for performing a planned movement and holding a desired posture. These skills can be modulated by nonspecific speed and compliance control signals without significantly disrupting their positional control. Speed and compliance rescaling without a loss of positional control make it possible to flexibly adapt the motor system to match the demands of a large range of tasks that would otherwise prove impracticable.

Another important function of such position-code invariance becomes apparent when we consider how speed and compliance control signals are strategically varied during skill acquisition (Gachoud et al. 1983; Humphrey and Reed 1983; Moore and Marteniuk 1986; Thelen and Fisher 1983). Early in the development of a skill, acts are typically performed with relatively low joint compliance (relatively high stiffness) and at low speed. As learning progresses, the learner speeds up and allows the limbs to become more compliant. This pattern constitutes an adaptive strategy because the final high-compliance, high-speed mode of operation is more energy- and time-efficient, whereas the initial low-compliance, low-speed mode insulates the learner from

large untoward consequences of miscalibrated position-control signals. For example, when learning to transport a glass of milk from table to mouth, a child performing at low speed will have time to halt, or correct on-line, misdirected actions, and low compliance will help prevent large terminal overshoots due to unexpected inertia. The low-speed, low-compliance parameter setting of the neuromuscular system defines a period during which the position-control system can receive the error feedback needed to learn skilled control of objects, while avoiding large, dangerous errors. Thus, the low-speed, low compliance period of juvenile behavior provides a kind of internal developmental 'scaffolding' that enables safe self-organization of skilled actions. Such internally generated scaffolding is an analogue of the external scaffolding prevalent in species whose adaptive strategy depends on an extended juvenile period of learning within a protective social environment (e.g., Bullock 1987).

Changing from the control strategy of high stiffness and low speed would be less effective if the skill learning that occurred during this training period were not transferable to the new control strategy of low stiffness and high speed. Transferability would be impaired if position-code invariance could be achieved only at particular values of speed and compliance. Thus neural circuits capable of position-code invariance at variable speed and compliance levels provide a basis for rapid skill development and generalization. Our neural models for trajectory formation and postural maintenance, which were developed in response to both physiological and psychophysical data, show how position-code invariance can be achieved without reliance on speed- or compliance-dependent learning.

2. Neural specification in the control of reaching

Though our results are more generally applicable, we focus herein on voluntary reaching movements and voluntary postural maintenance of the arm. To begin, consider the intrinsic relationships among arm muscle lengths, arm segment lengths, arm joint angles, and the position of the hand in space. Because the hand rides the end of the forearm segment, its position in space relative to the torso is determined by the lengths of the upper- and fore-arm segments, by the angles of the upper arm with the torso (shoulder joint angles), and by the angle of the
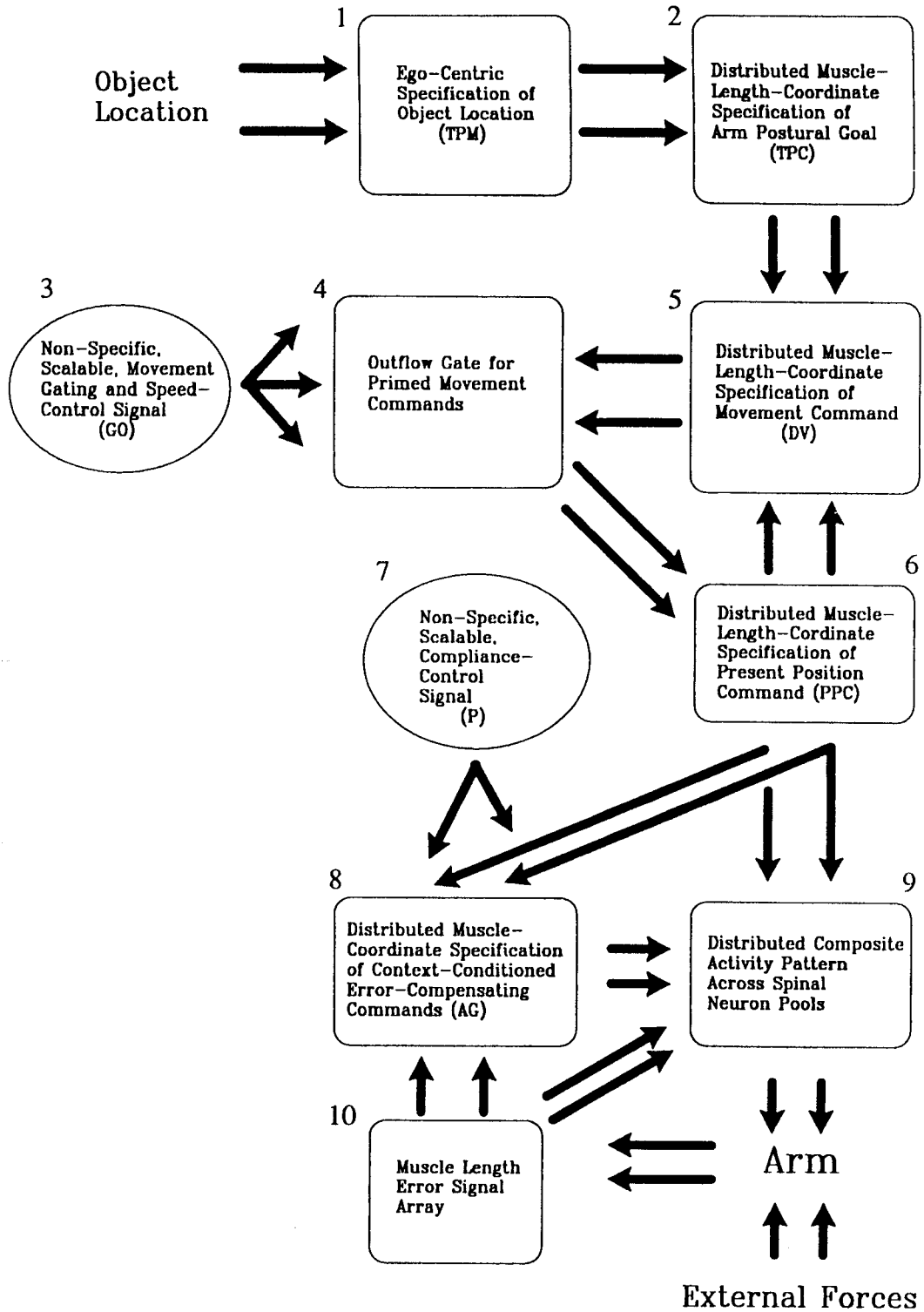
Fig. 1. Pattern-specifying signals (parallel arrows) as well as nonspecific, energizing signals (radiating arrows originating at sites 3 and 7) cooperate to provide flexible control of movement and posture. See text for details.

lower arm with the upper arm (elbow angle). The joint angles are in turn dependent on the lengths of the muscles that control rotations of arm segments at the joints. Thus, once limb segment lengths and muscle insertion points are given, any change in hand position can be described in terms of a set of muscle length changes. Corresponding to every realizable hand position there is at least one set of muscle length specifications which, if instated in the arm-controlling muscles, would move the hand to that position. The central nervous system can hereby indirectly control hand position by directly controlling muscle lengths.

To understand some of the issues associated with achievement of position-code invariances, consider fig. 1. In panel 6 of the figure, the Present Position Command, or PPC, codes hand position in muscle-length coordinates. The PPC is a pattern of neuronal activation levels distributed across a set of neuronal populations, each of whose activation levels rises when the muscle it controls is to be shortened and falls when its muscle is to be lengthened. If we associate the real variable PPC_i with each of these activation levels, where $i = 1, 2 \ldots n$ indexes one of n muscle control channels needed to control the arm, then the PPC is a vector with n components, $(PPC_1, PPC_2 \ldots PPC_n)$. This vector of real numbers corresponding to the pattern of activation levels serves as a natural 'muscle coordinate' code for present hand position, just as a three component (x, y, z) vector codes hand position in a Cartesian coordinate system. The multicomponent PPC generates out-flow movement signals to spinal neuron pools (panel 9) which in turn act on muscles capable of moving the arm.

Unfortunately, many factors threaten to disrupt an invariant linear relation between this array of commanded muscle lengths (PPC) and actual muscle lengths. First, external forces like gravity tend to rotate limb segments and thereby stretch or compress muscles to unintended lengths. Second, even in the absence of external forces, equal changes in the PPC specification are unlikely to cause equal changes in muscle length without significant auxiliary circuitry. This is because several sources of nonlinearity enter between the PPC stage and actual joint rotations. Even if the motor unit populations consisting of alpha-motoneurons and associated contractile fibers generated *forces* that were strictly proportional to descending neural input (which is not the case), joint rotations and muscle lengths ultimately depend on the *rotational* forces generated, i.e., on muscle torques. Torques depend both on developed muscular force and on the muscle's moment arm,

which changes as a function of joint angle. Finally, as shown in panel 7 of fig. 1, the PPC is not the only command signal directed toward the spinal neuron pools. Also impinging is a potentially disruptive signal intended to control joint compliance by simultaneously raising (or lowering) the contraction level of, and therefore the forces developed by, muscles pulling from opposite sides of the joint.

To compensate for the initially nonlinear response of arm muscles to PPC changes, it is necessary for the CNS to measure muscle length errors (panel 10) and to use error feedback to improve its performance. While such feedback supplies immediate *reactive* compensation (diagonal arrows from panel 10 to panel 9) via a stretch reflex, we suggest that it also guides learning in pathways capable of associating compensatory inputs with the specific contexts – such as particular PPC settings – in which compensations are needed. Such adaptive pathways afford *predictive* compensations that pre-empt errors. They are shown connecting panel 8 with panel 9 in fig. 1. Learning via such pathways is critical for what Bullock et al. (1991) have called *autonomous supercession of control*, a widely observed developmental phenomenon in which the control strategy utilized at an early stage of learning is autonomously superceded by a shorter, more efficient strategy as learning proceeds. In motor control examples, this often involves replacing iterative, feedback-corrected performances with less iterative performances based primarily on feedforward motor commands that were calibrated by learning during the prior, iterative performance phase. It is now well established that the cerebellum is one critical module for the learning of predictive movement-calibrating signals (e.g., Albus 1971; Grossberg 1969; Grossberg and Kuperstein 1986, 1989; Hore 1987; Ito 1984; Kawato et al. 1987; Marr 1969).

Although learned, error-preempting supplements to the PPC's input to the spinal motor pools are unavoidable in general, simulations summarized below suggest that the spino-muscular system is designed to automatically compensate for large variations in the compliance control signal even without learning. These compliance control signals are broadcast to the spinal neuron pools via the pathways from panel 7 through panel 8 to panel 9. The network model that served as the basis for these simulations is called the FLETE model (Bullock and Grossberg 1988d, 1989). The acronym FLETE stands for Factorization of LEngth and TEnsion, and the model includes a mathematical interpretation of many known aspects of the spino-muscular system (fig. 6),

which we believe has been shaped by evolution to ensure separable control of muscle length and muscle force despite the natural tendency of a muscle's force to covary with its length.

In particular, the FLETE model (sections 8–18) shows how joint compliance may be controlled independently of joint angle by merely adding the same co-contractive signal to both the outflow channels that eventually impinge upon the opponent motoneuron pools controlling muscles acting on opposite sides of a joint. Our analysis of the circuits that make this possible begins by showing that achieving a wide force range at each muscle length requires that motor units behave according to the size principle of motoneuron recruitment if muscle tissue is subject to yielding at high force levels. We then show that adding the same co-contractive signal to both outflow channels, in a system that obeys the size-principle of motoneuron recruitment, poses a threat to position-code invariance. This threat may be counteracted by appropriate use of efference copy feedback pathways in combination with reciprocal inhibition. *In vivo*, a pathway with appropriate properties is provided at the spinal segmental level by Renshaw cells and Ia interneurons. Thus the FLETE model, while achieving an important behavioral invariance property and thereby underscoring a strategy for motor skill development, also provides a new rationale for the size principle of motoneuron recruitment and for the opponent organization and parametric properties of the Renshaw-Ia efferent-copy feedback pathway. Finally, we show how ascending feedback signals arising from spindle organs can guide opponent cerebellar learning such that the total descending command to each opponent channel is simultaneously adjusted to compensate for moment-arm effects. This analysis predicts a confluence point for specific signals which control joint rotation and nonspecific signals which control joint compliance. The need to simultaneously adjust gains in both opponent channels also provides a computational rationale for fractured somatotopy in the cerebellum (Grossberg and Kuperstein 1986, 1989).

Other computational issues arise when we consider how to perform a reaching movement under the influence of a visual estimate of the location of an object to be touched. There must exist some mechanism for changing the Present Position Command (PPC) of panel 6 from its pre-reach value to a new Target Position Command (TPC) which, when instated peripherally as an actual pattern of muscle lengths, would juxtapose hand and object. Data of Bizzi et al. (1984) suggest that such

a PPC change is gradual and does not require visual feedback of hand position. In the VITE model, PPC updating is accomplished gradually by the ensemble of processes schematized in panels 1–6.

In panel 1, we assume that the visuo-motor system yields an egocentric specification of object location within a neural network called a Target Position Map or TPM (Grossberg and Kuperstein 1986, 1989; Nemire and Bridgeman 1987). This TPM specification is simply a firing pattern, distributed across one or more neural fields, that is specific to a given target locus relative to the body. By panel 2, an adaptive associative mapping has transformed the TPM specification into a TPC. The TPC, or Target Position Command, is a distributed neural pattern that specifies a vector of lengths, to which the arm-controlling muscles must contract in order to juxtapose hand and object. The associative mapping between TPM and TPC is adaptive because it must change as arm segments change their length during development. Because the hand rides the end of the arm, any change in arm segment length changes the geometrical meaning of a given TPC vector. Adaptive neural networks capable of learning a direct TPM → TPC coordinate transformation have been proposed recently by Kuperstein (1988) and by Ritter et al. (1989), but these models have not explained data about the mapping used by primates for eye-hand coordination (see Bedford 1989; Nemire and Bridgeman 1987; Soechting and Flanders 1989). Recent results on Vector Associative Maps (Gaudiano and Grossberg 1990, 1991, in press) promise to close this gap.

The descending TPC is compared at stage 5 with the motor vector ascending from stage 6. The latter is an 'efference copy' of the PPC. The comparison of the TPC with the PPC at panel 5 yields a Difference Vector, or DV, also in length coordinates, that specifies the muscle length changes required to move the arm from the PPC to the TPC. Thus the DV of panel 5 is the first specification so far mentioned that has the dimensions of a movement command.

Movement is not generated by directly adding the DV to the PPC. Instead, all components of the DV are multiplied by a nonspecific GO signal that is under voluntary control. The GO signal starts at zero before movement and then grows smoothly to a positive value as the movement develops. The site of the multiplication of the DV by the GO signal, depicted in panel 4, is called an outflow gate for primed motor commands. Until the GO signal becomes positive, outflow pathways from 5 through 4 to 6 are effectively 'gated shut.' Prior to

activation of the GO signal, a movement command (DV, panel 5) may be primed by instatement of a TPC (panel 2) different than the PPC (panel 6). The DV does not begin to be enacted until the site depicted in panel 3 begins to nonspecifically broadcast the time-varying GO signal. The rate of change of each PPC component, PPC_i, is proportional to the product of the GO signal multiplied by the DV component, DV_i. Thus the gating stage (panel 4) at which the GO signal multiplies the DV computes an estimate of movement velocity. Rescaling the GO signal synchronously modifies the contraction rate of all muscles contributing to the arm movement. The voluntary release of a primed movement, and the voluntary setting of movement rate, are thus both controlled by the nonspecific GO signal.

Components 2–6 of fig. 1 comprise the VITE model for variable-speed trajectory formation (Bullock and Grossberg 1986, 1988a, 1988b, 1988c, 1989). The acronym VITE stands for 'Vector Integration To Endpoint' to contrast its operation with simpler spring-to-endpoint models of trajectory formation (e.g. Cooke 1980). The VITE model's DV specifies the residual distance through which each muscle must contract before the limb can reach the desired terminal posture. The model's mathematical formulation (section 3) explains how to design a central pattern generator using efference copy feedback to ensure that the entire array of muscle synergists controlled by the DV may be influenced by a speed-control GO signal in such a way that all muscles tend to complete their contractions synchronously and accurately despite: mid-course changes in desired movement endpoint, different contraction amplitudes for each muscle, different contraction onset-times for each muscle, and different overall movement speeds. Despite its simplicity, the VITE model has now been successfully used (Bullock and Grossberg 1988a, 1988b, 1989) to explain a considerably wider range of physiological and kinematic data than alternative theories (see sections 5 and 6).

In summary, the VITE and FLETE circuits are components of a modular theory of intentional motor control, some key aspects of which are schematized in fig. 1. The theory seeks to provide a rigorous basis for understanding the interdependent nature of computations distributed across several neural sites heretofore treated separately. The two modules treated in this paper illustrate how invariant yet flexible positional control may be assured with a minimum of compensatory learning if careful use is made of efference copy feedback in conjunc-

tion with nonspecific speed and compliance modulating signals that are suitably nested within an opponently organized motor command system. Without such invariance properties at low levels of the motor control system, acquisition of skills with significant hierarchical structure (e.g. Fischer 1980), such as tool manipulation and speech, would be more protracted, and the cultural modes of adaptation based on such skills could less easily evolve. The following sections focus on the computational bases of the cited invariance properties.

3. Position-code invariance under speed rescaling in a VITE circuit

Fig. 2 schematizes the organization of two of n muscle-length control channels within a VITE circuit (compare panels 2–6 of fig. 1) and shows the type of differential equations used to simulate the circuit. Because a single muscle cannot both pull and push, each fig. 2 channel requires an opponent, or push–pull, microstructure like that shown in fig. 3. To simplify the exposition, we will consider the units in fig. 2, and we let $TPC_i = T_i$, $DV_i = V_i$, and $PPC_i = P_i$. Although we consider only one channel in the following discussion, the results hold for all channels within which updating is controlled by a shared GO signal, G.

We now explain how T_i can update P_i with a positional accuracy that is relatively insensitive to variations in the size of G. Consider a

$$\frac{d}{dt}V_i = \alpha(-V_i + T_i - P_i)$$

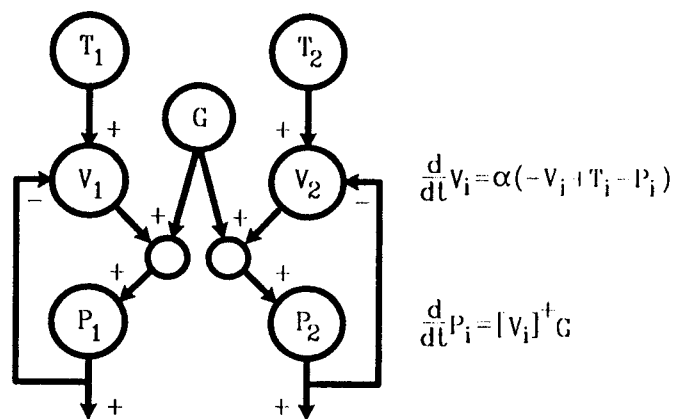$$\frac{d}{dt}P_i = [V_i]^+ G$$

Fig. 2. Updating rates within all component channels of a VITE circuit are influenced by a common, multiplicative GO signal. Variable key: T_i = target position command; V_i = difference vector; G = GO signal; P_i = present position command. Opponent interactions that exist between agonist and antagonist sub-channels within each depicted channel are shown in fig. 3.
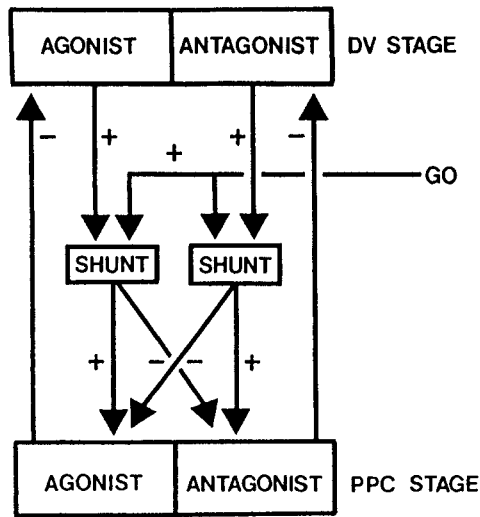
Fig. 3. Opponent interactions among VITE circuit sub-channels controlling agonists and their antagonists enable coordinated, automatic updating of their present-position commands (PPCs). Outputs from the PPC stage serve as the basis for reciprocal control of opponent muscles' contractile states. The term shunt refers to a multiplicative interaction between neural variables.

typical case in which initially $T_i > P_i$, which creates a positive difference vector component, V_i. When G becomes positive, the gate between the cellular site registering activity V_i and the cellular site registering activity P_i is opened and updating of P_i begins. As shown in fig. 2, the time rate of change of P_i, $(d/dt)P_i$, is given by the product $[V_i]^+ G$, where notation $[V_i]^+$ means $\max(V_i, 0)$. This product rule implies that whenever V_i becomes zero, so will the updating rate $(d/dt)P_i$, regardless of the value of G. Moreover, because of the inhibitory effect of P_i on V_i, V_i is driven toward zero as P_i is updated towards T_i. Thus the product rule in conjunction with inhibitory efference-copy feedback assures that updating will self-terminate when $P_i \approx T_i$ even if G is much greater than 0. This is most of the story of position-code invariance across different settings of G.

However, the size of G can cause positional errors which help to explain the classical Fitts Law (Fitts 1954) and Woodworth's Law (Woodworth 1899). Given *any* finite value of the averaging rate α at which V_i integrates $T_i - P_i$ (fig. 2), $V_i(t)$ takes some time to react to changes in $P_i(t)$. In particular, even if $P_i(t) = T_i$ at a given time $t = t_0$, $V_i(t)$ will typically require some extra time after $t = t_0$ to decrease to the value 0, and $P_i(t)$ will continue to increase during this extra time. If α is very large, $V_i(t)$ can approach 0 quickly. Consequently, $V_i(t)$ will

not allow $P_i(t)$ to overshoot the target value T_i by a large amount. On the other hand, given *any* choice of α, the *relative* amount whereby $P_i(t)$ overshoots the target T_i depends upon the size of the GO amplitude G. This is true because a larger value of G causes $P_i(t)$ to increase faster, and thus $P_i(t)$ can approach T_i faster. In contrast, $V_i(t)$ can only respond to the rapidly changing values of $T_i - P_i(t)$ at the constant rate α. As a result, $V_i(t)$ tends to be larger at a time $t = t_0$ when $P_i(t_0) = T_i$ if G is large than if G is small. It therefore takes $V_i(t)$ longer to equal 0 after $t = t_0$ if G is large. Thus $P_i(t)$ overshoots T_i more if G is large. This covariation of amount of overshoot with overall movement velocity is a speed–accuracy trade-off.

These remarks indicate that position code invariance is achieved only approximately. The VITE model circuit can generate positional errors whose sizes depend on network parameters such as the rate α at which V_i integrates $T_i - P_i$ and the rate G at which P_i integrates $[V_i]^+$. Computer simulations and mathematical theorems reported in Bullock and Grossberg (1988a) proved that these errors obey Fitts' Law and Woodworth's Law. These analyses thus explained these Laws as emergent properties of a network designed to generate synchronous multi-joint goal-directed movement trajectories at variable speeds.

4. Multiplicative gating in variable-speed synchronous trajectory formation

The behavioral property of multi-joint synchrony at variable speeds is based upon the neural property that the GO signal multiplies the DV components. If, instead, G were added to each V_i the relative updating rates for different muscles would no longer be proportional to the relative amounts by which they must contract. In particular, muscles needing to contract through greater distances would take longer times to do so, and the resultant movements could change direction in an uncontrolled fashion in mid-course.

In contrast, the VITE model's multiplicative $(DV) \cdot (GO)$ rule leads to a robust synchrony property, such that muscles contracting through different lengths can complete their contractions in equal time. Fig. 4 illustrates the wide operating range of this synchrony property. When all DV_i components are switched on at the same time and multiply the same GO signal, then all components complete their movement syn-

⊥ SYNERGIST BEGINS CONTRACTION
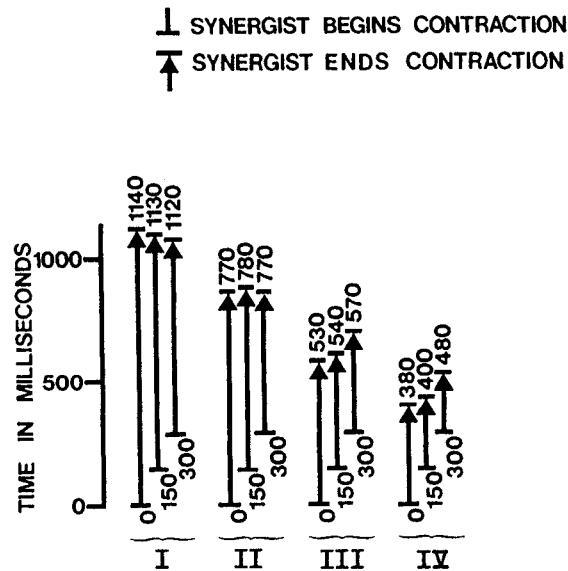
⊤ SYNERGIST ENDS CONTRACTION

Fig. 4. Simulation results showing contraction offset times for three synergistic muscles with different onset times, as a function of the GO signal scalar (the voluntarily chosen multiplier of the time-varying GO signal). In each block, the DV component corresponding to muscle one begins to be read out 0 ms after the start of GO signal buildup, muscle two 150 ms after the start of GO buildup, and muscle three 300 ms after the start of GO buildup. The GO signal scalar was 10, 20, 40, and 80 in blocks I–IV, respectively. Results indicate automatic VITE circuit compensation for staggering of contraction onset times.

chronously no matter how the GO signal is chosen. This synchrony property was proved mathematically in Bullock and Grossberg (1988a). When different DV_i components are switched on at different times and multiply the same GO signal, then their onset times may be deferred by as much as 50 percent of the total movement time without significantly disrupting offset synchrony. This latter synchrony property is strengthened when the GO signal starts at zero and grows gradually during movements (see fig. 5a, b). Then later-starting DV_i components interact with a GO signal which has a larger average size during their interval of integration.

This staggered-equifinality property may be as important for rapid skill development as the position-code invariance property. In particular, Hollerbach et al. (1986) have suggested that staggered onset times may be needed to generate nearly straight hand trajectories despite movement planning in muscle-length, or joint-space, coordinates. In addition, offset synchrony is needed to learn and perform movement

sequences in which gesture *n* is rapidly succeeded by gesture *n* + 1, as in rapid speech and typing. Without offset synchrony, it would be difficult to precisely predict the time when any gesture would be completed, hence also difficult to predictively control onset of the succeeding gesture without risking interference from a lagging component of the prior gesture. The VITE network reconciles staggered onsets with synchronous offsets by the simple device of a continuously growing GO signal.

5. Recent neural and behavioral evidence for the VITE model

This section summarizes some of the experimental evidence that has come to our attention since the extensive summary of data we completed in October, 1986 when our first journal article on the VITE model was submitted (Bullock and Grossberg 1988a). We emphasize evidence for two key predictions of the model: the existence of a multiplicative GO signal, and the existence of a duration-dependent asymmetry in velocity profiles.

Because the VITE model proposes that trajectories are generated as the arm tracks the evolving state of the PPC, the model can be tested in two ways: by comparing trajectories of the neural circuit's output stage (e.g., fig. 5) with behavioral data concerning actual arm trajectories, and by checking for the existence of the neural components, including the PPC, that are postulated in the model. Detailed quantitative comparisons of model predictions with behavioral data can be found in Bullock and Grossberg (1988a, 1988b). Among the properties treated therein are: peak acceleration as a function of movement amplitude and duration, and isotonic arm movement properties before and after arm-deafferentation in animals deprived of visual feedback (Bizzi et al. 1984); synchronous and compensatory 'central error correction' properties of isometric contractions (Gordon and Ghez 1987); velocity profile invariance across different movement distances (Freund and Büdingen 1978); duration-dependent velocity profile asymmetries and the invariant ratio between peak velocity and average velocity in speech and arm movements (Beggs and Howarth 1972; Ostry et al. 1987; Nagasaki 1989; Zelaznik et al. 1986); and velocity amplification following target-switches in speech and arm movements (Georgopoulos et al. 1981; Abbs et al. 1984).

Neurophysiological data support the existence of the major stages in the VITE model. In particular, the VITE model includes a DV stage, the analogue of which does not exist within mass-spring models of trajectory formation (e.g., Cooke 1980). Cell populations have been identified that possess all the properties required of an *in vivo* analogue of DV stage neurons. For example, Georgopoulos and associates (Georgopoulos et al. 1984a; Schwartz et al. 1988) have located a class of cells in the shoulder-elbow zone of the precentral motor cortex (area 4). Called vector cells, they have the following properties in common with VITE model DV cells: (1) activity levels correlate with arm movement direction but not arm movement endpoint; (2) activity levels may be primed prior to movement, as required by the postulate that actual movement depends on GO signal activation; (3) the time course of vector cells is highly correlated with the time course of the model DV; (4) vector cell coding of movement direction does not reverse during the second half of the movement, indicating pure kinematic coding with no braking-force component; and (5) vector cells project to interneurons rather than directly to motoneurons, as required by the VITE model postulate of an outflow PPC stage that must be supplemented by additional signals, such as FLETE model signals, to generate the total movement command. Thus the VITE model provides a mechanistic understanding of how the neural population vectors measured by Georgopoulos and associates may be computed by a distributed neural circuit. The TPC is likely to be computed in the posterior parietal cortex. Evidence for a GO signal generator in the globus pallidus will now be summarized.

An *in vivo* candidate for a GO signal pathway must pass four tests. First, stimulation at some site in the proposed pathway must have an effect on the rate of muscle contractions. Second, it must have this effect without affecting the amplitude of the contractions. Thus stimulation should have no effect on movement accuracy, except possibly for effects caused by imperfect motor realization of the PPC commands. Third, this rate-modulating effect should be nonspecific: it should affect all muscles that are typically synergists for the movement in question. Fourth, because movement depends on the conjunction of a positive DV and a positive GO signal, no movement should occur in the absence of either signal.

Studies conducted by Horak and Anderson (1984a, 1984b) have supplied data that support all of these properties. Horak and Anderson

(1984a) showed that 'when neurons in the globus pallidus [of Macaque monkeys] were destroyed by injections of kainic acid (KA) during task execution, contralateral arm movement times (MT) were increased significantly, with little or no change in reaction times' (p. 290). This satisfies the *rate criterion*. The rate of motor recruitment was depressed 'in all the contralateral muscles studied at the wrist, elbow, shoulder, and back, but there were no changes in the sequential activation of the muscles' (p. 20). This satisfies the *nonspecificity criterion*. 'Animals displayed no obvious difficulty in aiming accurately ... they did not miss the 1.5-cm target more often following KA injections, and there was no noticeable dysmetria around the target' (p. 300). This satisfies the *accuracy criterion*.

Horak and Anderson (1984b) used an electrical stimulation paradigm instead of a lesion paradigm. They found that 'stimulation in the ventrolateral internal segment of the globus pallidus (GP_i) or in the ansa lenticularis reduced movement time, whereas stimulation at many sites in the external pallidal segment (GP_e), dorsal GP_i, and putamen increased movement times for the contralateral arm' (p. 305). Once again, these effects were nonspecific: 'no somatotopic effects of stimulation were evident. If stimulation at a site produced slowing, it produced a depression of activity in all the muscles studied. Even stimulus currents as low as 25 μA affected proximal as well as distal muscles, flexor as well as extensor muscles, and early- as well as late-occurring activity' (p. 309).

The *conjunction criterion* for a GO-signal pathway was also met. In the VITE model, activation of the GO-signal pathway produces movement only if instatement of a TPC different from the current PPC leads to the computation of a non-zero DV, regardless of the value of *G*. In agreement with this property, Horak and Anderson (1984b) observed that 'stimulation at sites that speeded movements did not induce involuntary muscle activation in resting animals nor did it change background EMG activity prior to self-generated activity during task performance' (p. 313). In Bullock and Grossberg (1988a) we noted that 'very rapid freezing can be achieved by *completely* inhibiting the GO signal at any point in the trajectory'. This property of the model was partially shown to be a property of the GP system by the demonstration, noted above, that stimulation in inhibitory zones adjacent to GP_i significantly slowed movement. Horak and Anderson also reported that 'stimulation with 50 or 100 μA at ... sites ventral and medial to

typical GP_i neuronal activity completely and immediately halted the monkey's performance in the task' (p. 315). Though the sites producing halting in the Horak and Anderson studies apparently do not inhibit the GP_i, they may inhibit targets of the GP_i output pathway. Prior studies using much larger currents in zones known to inhibit GP_i have produced halting (Van Buren et al. 1966). Taken together, their experiments led Horak and Anderson (1984b) to conclude that 'the basal ganglia ... determine the speed of the movement' (p. 321). Consistent rate-control data for speech movements have been reported by Mateer (1978).

In a study of timing relations between natural pallidal neuron discharges and the earliest detectable EMG activity, Anderson and Horak (1985) observed that though about 30% of pallidal neurons began firing 50–150 ms before mechanically detectable movement, 'only 13 of 108 neurons showed changes in activity before the earliest EMG activity recorded during the same trials, and for only two of them did the initial changes in firing rate precede the initial changes in EMG activity by more than 25 ms' (p. 444). From this they concluded that 'it is unlikely that changes in pallidal firing would be important in determining the initiation of the arm movement ... but they could be important in controlling the buildup or scaling of EMG activity and thus the duration of the movement' (p. 444). Similar timing relations in monkeys have been reported by Mitchell et al. (1987).

These timing relations have several alternative interpretations that require further discussion, especially in the light of cat data consistent with an initiating role for pallidal output signals (Neafsey et al. 1978). Both theoretical and empirical considerations suggest that Anderson and Horak may have underestimated the role of the GP_i in movement initiation. In any planned movement context, there are likely to be a set of central events, all of which may be jointly involved in 'determining the initiation of the arm movement'. In particular, an arm movement will be more successful if the muscles controlling body segments that serve as the postural base for the arm are activated before the phasic arm movement is itself initiated. Gahery and Massion (1985) have reported central and muscular postural adjustments with lead times in excess of 25 ms before the onset times for central and muscular arm-movement producing activations.

From this perspective, the data of Anderson and Horak do not rule out the GP_i as the output stage of a GO signal generator. Rather, they

further buttress the argument that a gradually increasing GO signal exists in the GP_i. In particular, each animal individually showed some pallidal activity at least 25 ms prior to the earliest EMG activity. Close inspection of Anderson and Horak's (1985) fig. 8 reveals that this 'short' 25 ms lead time held only for the thoracic paraspinal muscle, whose activity was probably generated by the separate circuit responsible for preparing the postural base for the forthcoming arm movement (Gahery and Massion 1985). In contrast, pallidal activity led EMG activity in all arm-projection muscles (biceps, deltoid, radialis) by at least 50 ms. Such a lead time is compatible with an initiating role because the GP_i may be tri-synaptically linked to motoneurons via two separate pathways.

In addition, Anderson and Horak used a simple RT task, which allows complete DV priming before onset of the GO signal. Such a task would be expected to eliminate any effect of the GO signal on RT as well as reduce to a minimum the lag between GO activation and initial muscle activation. Initial muscle activity in the model is affected by the product of the GO signal and the large initial DV. Because the GO signal is assumed to start small and to grow gradually, only a small proportion of pallidal neurons should become active prior to initial muscle activity. Thus the Anderson and Horak (1985) observations of gradual recruitment of active pallidal neurons are consistent with the hypothesis of a gradually growing GO signal. This hypothesis also helped to quantitatively explain a variety of data about arm movement velocity profiles in Bullock and Grossberg (1988a). The Anderson and Horak paradigm provides an opportunity to make a direct neurophysiological test of whether a gradually growing GO signal helps to reconcile staggered onset times with near-synchronous offset times. Are nearly straight reaching movements with widely staggered onset times rendered less controllable by rapid onset of pallidal activity caused by direct electrical stimulation?

Because the internal segment of the globus pallidus is one of two main output nuclei for the basal ganglia (BG), an assessment of its suitability as a GO signal generator needs to consider inputs to the basal ganglia. Do the basal ganglia receive the afferents one would expect to govern the final decision to execute a primed motor command? This issue has recently been addressed by Passingham (1987), who concluded 'that it is the basal ganglia that finally direct the action to be taken' (p. 90). Regarding BG inputs, he noted that for a correct

evaluation of the context for action, 'the motor system must be influenced by information from all of the cortical regions ... In fact there is a massive projection from all these areas, but it runs not across the cortex but downward to the basal ganglia' (p. 85). Moreover 'the ventral striatum [one of the BG input zones] receives a heavy projection from the amygdala ... [which] plays a crucial role in the learning of motivational and emotional associations (p.85).' Thus the basal ganglia do receive inputs whereby cognitive and motivational information may be integrated to arrive at decisions to act. These convergent pathways to the basal ganglia support the interpretation of the GO signal as 'the will to act'. No 'will' implies a zero GO signal. When a positive 'will to act' can be continuously modulated, it provides a basis for variable-speed control.

The other main output nucleus of the basal ganglia – the substantia nigra (SN) pars reticulata – is known to gate read-out of movement commands controlling saccadic eye movements. It does this by disin-hibiting deeper layers of the superior colliculus (Sparks and Jay 1986; Wurtz and Hikosaka 1986). Grossberg and Kuperstein (1986, 1989) have modeled how this gating action enables planned and attentionally modulated eye movement commands to effectively compete with more rapidly computed visually reactive eye movement commands to decide which type of information will determine where the eye looks in any given situation. In baboons, SN lesions produced a marked increase in the duration of a forelimb pointing movement without causing a change in movement accuracy, and the slowing involved the whole trajectory (Viallet et al. 1983), consistent with VITE model equations.

Further data relevant to the existence of a GO-signal pathway were recently reported by DeJong et al. (1990). Continuous response mea-sures taken during a choice RT study of control processes underlying response inhibition revealed 'that responses could be interrupted at any time' (p. 164). When considered in the context of other experimental results, this finding led them to conclude that 'the distinction between a central and a peripheral inhibitory mechanism is also consistent with the distinction between central processes, concerned with the program-ming of the movement, and more peripheral processes, involved in the initiation of the movement and the control of its speed, proposed by Bullock and Grossberg (1988) in their model for the control of limb movements' (p. 179).

Another prediction of the VITE model can be seen in the simulation

results summarized in fig. 5. The model implies that velocity profiles should not be perfectly bell-shaped. Instead they should deviate from symmetry in a direction that depends on movement duration. Short duration movements should have a longer accelerative than decelerative portion – 'left-tail asymmetry' – whereas long duration movements should have a longer decelerative than accelerative portion – 'right-tail asymmetry'. Though their data were not presented in such a way as to make the effect easy to see, we noted in Bullock and Grossberg (1988a)
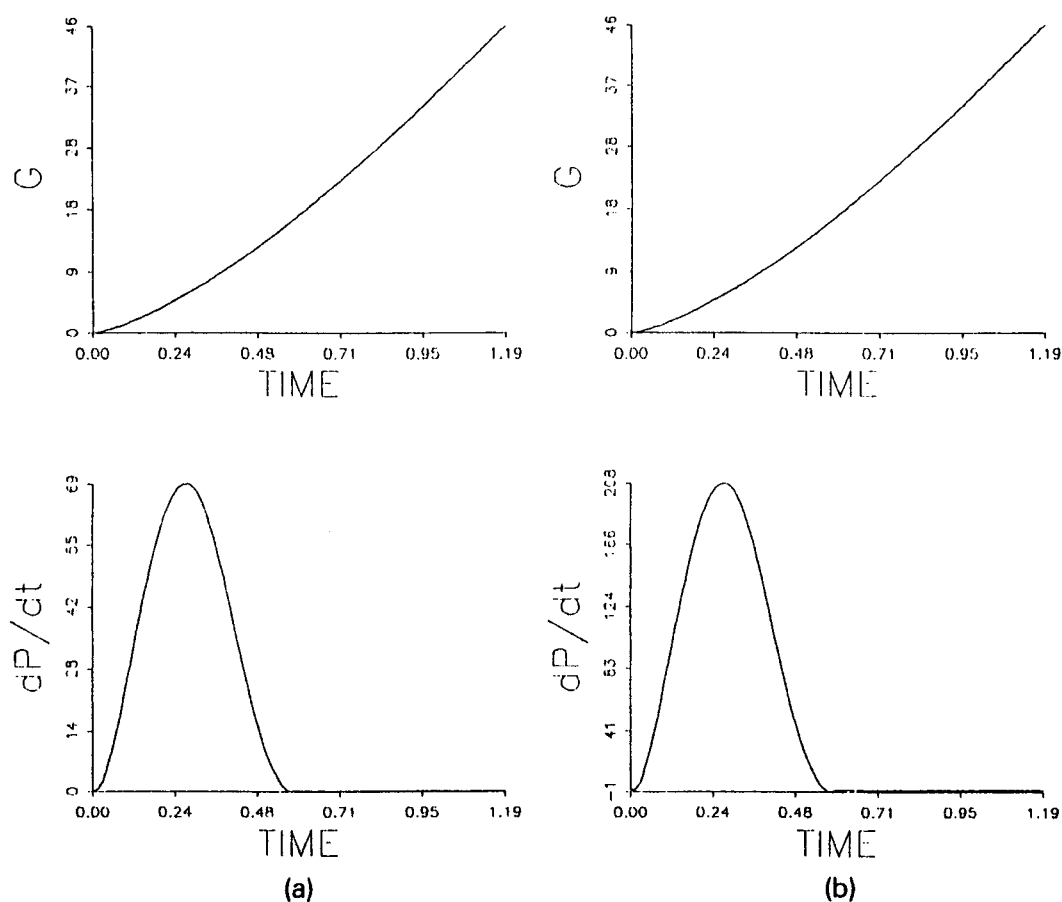

Fig. 5. (a, b): With equal GO signals, movements of different size have equal durations and perfectly superimposable velocity profiles after velocity axis rescaling. Shown are GO signals and velocity profiles for 20 and 60 unit movements lasting 500 ms. (c, d, e [see p. 24]): Velocity profiles associated with small, medium, and large GO magnitudes result in slow, medium, and fast performance of a 20 unit movement. Each SR value gives the trajectory's *symmetry ratio*; that is, the time taken to move half the distance divided by the total movement duration. These ratios indicate progressive symmetrization at higher speeds, within the range of speeds shown. (f [see p. 24]): The velocity profiles shown in (c), (d), and (e) are not perfectly superimposable after time and velocity normalization.
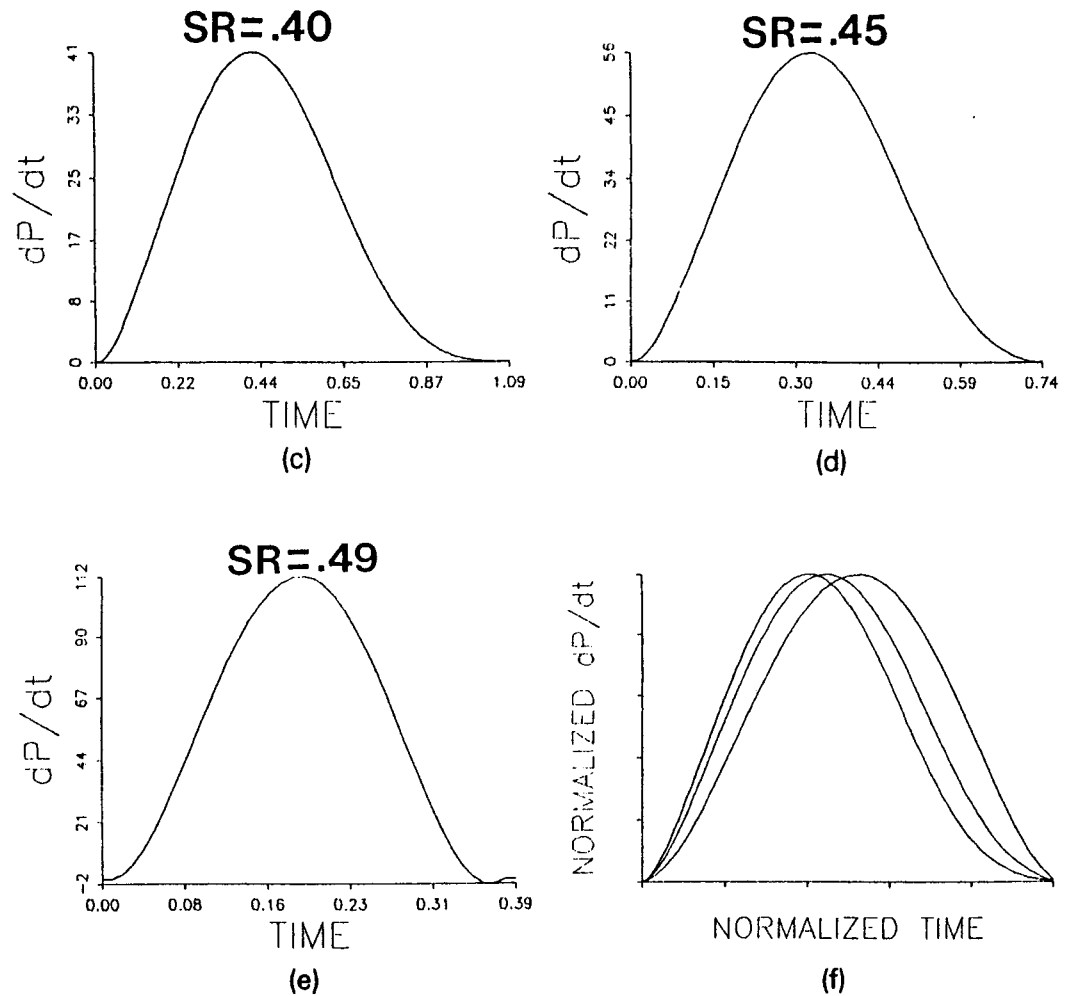
Fig. 5 (continued).

that Beggs and Howarth had presented consistent data on right-tail asymmetry in 1972. Further data documenting both predicted types of duration-dependent asymmetry have now been reported by a number of researchers: Zelaznik et al. (1986) and Moore and Marteniuk (1986) for rapid arm movements, Ostry et al. (1987) for orofacial (speech and nonspeech) and arm movements, and Nagasaki (1989) for a full speed-range of arm movements.

Nagasaki's results are particularly relevant because he compared his data both to predictions of our model and to predictions of various optimization models of trajectory formation, including variants of the minimum jerk model of Hogan (1984) and the minimum effort model of Nelson (1983). He noted that 'Bullock and Grossberg (1988a) also

predicted the same type of asymmetry as ours, though they could not verify their theoretical results ... because of the lack of available data. Their model is constructed on a fundamentally different basis from optimization theory; it needs no explicit preprogramming of movement kinematics ... Our constrained jerk model assumed that the ballistic and slow movements were controlled so as to reduce the abrupt change in acceleration at the start and end of the discrete movements. The actual movements, however, did not satisfy the minimum-cost thereby introduced' (p. 325). More generally, Nagasaki concluded that to reproduce the duration-dependence predicted by the VITE model and observed in his data, 'it would be necessary to examine cost functions other than jerk or effort for ballistic or slow movements.' In Bullock and Grossberg (1988b), we showed that the VITE model also greatly outperformed both minimum jerk and minimum effort models in predicting the peak accelerations measured by Bizzi et al. (1984).

Two other recent developments also deserve mention. Ebner (1989) has reported cells in premotor cortex whose activity during arm movements is correlated with motor error, i.e. the residual distance to target, as are model DV cells. Soechting and Flanders (1989) have used a 'blind reaching' paradigm, in which subjects made reaches to visually-specified targets without on-line visual guidance, to draw conclusions consistent with VITE model properties. In particular, they concluded that 'once target location is represented in body-centered coordinates, arm movement to a target could be achieved in principle by means of one transformation: mapping from target location to an appropriate level of activation of each of the limb muscles ... Once both the initial and final positions are represented in terms of joint angles, it is possible to derive the direction and amplitude of the movement required to attain the target by taking the vectorial difference' (p. 606).

6. Target switching during movement sequences

By supporting VITE model predictions regarding separate DV and GO signal processes, the data of Georgopoulos et al. and Horak and Anderson also support the more general hypothesis that motor systems, like sensory systems, implement factorization of pattern and energy (section 1). In the VITE component, this factorization means that a movement's speed ('energy') can be scaled up or down over a wide

range without disrupting the movement's direction or spatial endpoint ('pattern'). By using a GO signal that grows gradually during the movement time (fig. 5a, b), all synergists complete their contractions at approximately the same time even if movement onset times of different synergists are staggered by a large amount (fig. 4). These properties of the model, together with the strong evidence for separate DV and GO signal pathways *in vivo*, provide a basis for understanding how primates can achieve space-time equifinality – all synergists reaching their length targets at equal times – yet retain separate control of rate and position. Rate-control models relying on *static* stiffness adjustments (e.g., Cooke 1980) lack this temporal-equifinality property.

A closely related property of the VITE model gains importance during the many occasions when the TPC is updated one or more times during a movement or movement sequence. This may occur, for example, if the position of the object to be reached unexpectedly changes. Alternatively, a subject reaching for an object that is initially in the visual periphery may make a better estimate of object location after performing a saccadic eye movement to foveate the object. Saccades take less time than an arm movement that may be unfolding in parallel. In either case, the TPC and DV are rapidly updated, and this late-arriving information affects the arm's trajectory more quickly because the GO signal is already fully developed. Thus the factorization of TPC and GO signal, along with the hypothesis of a gradually growing GO signal, implies that a higher peak velocity will be achieved as a result of a mid-trajectory switch in TPC. Such an amplification of velocity facilitates reaching the target after the incorrect initial TPC is updated. This speed-up occurs 'on-the-fly' as the effects of the perturbation flow through the system via dynamic real-time computations. Georgopoulos et al. (1981) have reported such an increase of peak velocity during target-switching experiments in monkeys.

An experiment by Goodale et al. (1986), analogous to the Georgopoulos et al. (1981) study with monkeys, showed that humans also possess the ability to compensate for in-course target switches. Their experiment was also consistent with an explanation in terms of TPC updating and flow-through, because they eliminated the possibility that corrections could be based on visual comparisons of the relative positions of hand and target. In particular, compensations to a change in target position occurred in the arm's trajectory even when the arm and hand were invisible to the subject.
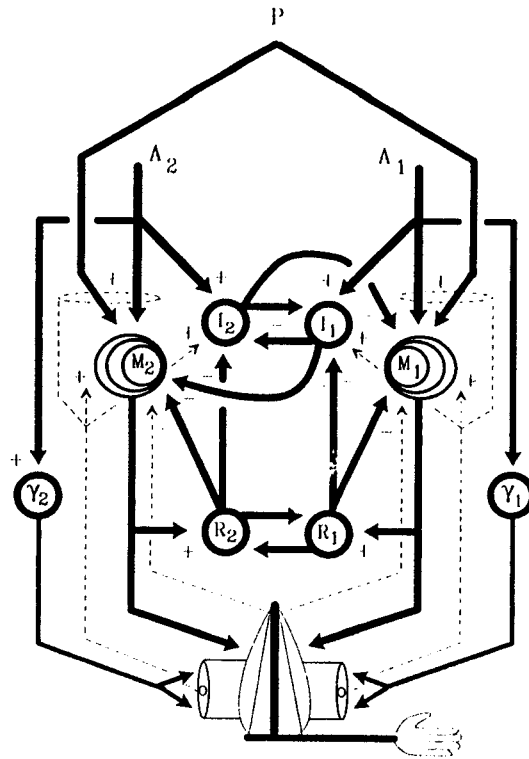
Fig. 6. FLETE model components: Neuron populations comprising two channels control opponent muscles acting on a joint. Descending signal P to both channels allows co-contraction and joint stiffening. Adjusting the balance between descending signals A_1 and A_2 allows reciprocal contractions and joint repositioning. For clarity, subpopulations of neurons and some signal pathways are not depicted. Key: I_i = Ia interneuron population in channel $i, i = 1,2; \gamma_i$ = gamma motoneurons; $M_i = \alpha$ motoneurons; R_i = Renshaw cells; + = excitatory input; − = inhibitory input.

Fisk and Goodale (1988) have offered an interpretation of late-occurring in-course error corrections, also proposed by Cooke and Diggles (1984), that is consistent with VITE model mechanisms. They concluded that many terminal error corrections are not based on either proprioceptive feedback from the limb or on visual comparisons of the relative positions of hand and target. Rather, such corrections are based on a comparison made between an internal representation of the target's locus and an internal representation of the hand's estimated location based on movement commands. These results support the VITE model as well as the classical hypothesis that even infants typically perform reaches without needing to compare the position of their seen hand with the seen target (Piaget 1963).

7. From kinematics to dynamics: generating forces to ensure that the arm tracks the evolving PPC

The VITE circuit places stringent requirements on other components of the sensory-motor system because it requires continuous or near-continuous adjustment of the balance of forces acting on the limb to ensure that the limb tracks the evolving PPC without significant lags or overshoots. Some of these components are modeled herein to explain how they autonomously generate the force-time patterns required to track VITE-generated trajectories. When both types of circuits are understood, a quantitative mechanistic understanding of the two of the most fundamental problems in sensory-guided motor control would then be approached: how to generate continuously modifiable kinematic plans, and how to generate the continuously modifiable force-time patterns needed to realize them.

8. FLETE: an opponent spino-muscular model for factorization of length and tension

We now address position-code invariance under compliance rescaling. The key problem is how the nervous system ensures independent control, or Factorization, of the LEngth and TEnsion of muscles controlling a movable limb, hence the acronym, FLETE, of our model. We report simulations that show how an opponently organized spino-muscular system (fig. 6) may use co-contraction to vary limb compliance without causing joint rotations by inadvertently changing the lengths of opponent muscles.

9. Wide force range at each muscle length requires size principle

Consider the forces, F_i, $i = 1, 2$ developed by two muscles operating on different sides of a joint. In a springy tissue like muscle, developed force depends on the amount of stretch beyond the resting length. Because muscle can actively contract, muscle has a *variable* threshold length for force development (e.g., Feldman 1986). These properties can be approximated by

$$F_i = g\left(\left[L_i - \Gamma_i + C_i\right]^+\right),\tag{1}$$

where L_i is muscle length, Γ_i is the resting muscle length, C_i is the amount of contraction, and function $g(w)$ is monotone increasing. Notation $[w]^+$ means $\max(w, 0)$. Thus eq. (1) says that whenever the sum of L_i and C_i exceed Γ_i, the muscle generates a force whose magnitude increases as L_i or C_i become larger.

Because contracted fibers relax after each neurally elicited twitch and *yield* when the force acting to stretch them is sufficiently large (Houk and Rymer 1981; Partridge and Benton 1981), a simple law for C_i is

$$\frac{d}{dt} C_i = \beta_i [(B_i - C_i) M_i - \delta C_i] - [F_i - \Gamma_F]^+, \tag{2}$$

where $0 < \beta_i < 1$ and M_i is the output signal of the ith alpha-motoneuron pool. As M_i grows, it activates more contractile fibers up to the limit set by B_i. Parameter δ specifies the fiber relaxation rate. When force F_i exceeds threshold Γ_F, which may happen when an external or antagonist muscle's force opposes muscle shortening, it reduces contraction. By constraining β_i to be between 0 and 1, contraction caused by neural input M_i is assured to be slow relative to the decontraction or 'yielding' produced by external or already developed antagonist muscle forces. The kind of functional relation among force, muscle length, and contractile state created by eqs. (1) and (2) is schematized in fig. 7.

At equilibrium, $(d/dt)C_i = 0$ in (2), so the equilibrium value of C_i is

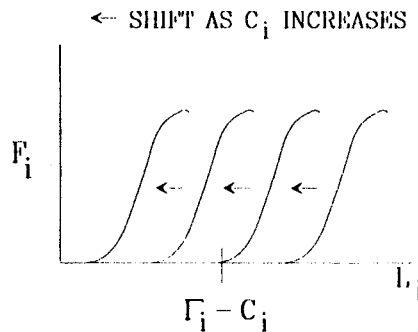$$C_i = \frac{M_i B_i - \dfrac{[F_i - \Gamma_F]^+}{\beta_i}}{M_i + \delta}. \tag{3}$$

Fig. 7. In first approximation, the effect of increased muscle stimulation is a shift in the threshold length for force development.

Given (3), how is it possible to generate and sustain forces much larger than Γ_F at a fixed muscle length? By (1), greater force at a fixed length L_i can be generated only by increasing C_i. However, if β_i is constant and less than 1, then (3) shows that the negative force feedback will cancel the effects of increasing M_i, and C_i will not grow large. To overcome this deficiency, let the contraction rate parameter β_i and the number of contractile fibers B_i increase with M_i. Such a relation has been well-documented empirically, and is called the *size principle* of motor unit organization (Hennemann 1957, 1985): as total excitatory input to the alpha motoneuron population grows, it recruits additional, progressively larger motoneurons which have faster conducting axons, whose collaterals reach many more motor fibers and whose potentials evoke more rapid muscle contractions. Eq. (3) provides a more complete functional perspective on the size principle by emphasizing the importance of contractile rate for the achievement of large force magnitudes.

10. Size principle with co-contraction pose a threat to position-code invariance

However, the size principle, which helps decouple length and force variation, can pose a threat to position-code invariance. To see how, suppose that the CNS controls equilibrium muscle lengths by setting the relative sizes of inputs A_1 and A_2 to motoneurons in opponent muscle control channels 1 and 2, respectively. If a limb segment is initially at equilibrium with $F_1 = F_2$, then by (1),

$$g\left(\left[L_1 - \Gamma_1 + C_1(A_1)\right]^+\right) = g\left(\left[L_2 - \Gamma_2 + C_2(A_2)\right]^+\right), \tag{4}$$

where $C_i(A_i)$ denotes the equilibrium value of C_i when $M_i = f(A_i)$ in (2). Now try to hold the limb at the same position, but more rigidly, by increasing the level of muscle contraction on both sides of the joint. The simplest way to do this is to add a constant P to each motoneuron input (Humphrey and Reed 1983). Then $M_1 = f(A_1 + P)$ and $M_2 = f(A_2 + P)$. However, in a system that obeys the size principle, (4) implies

$$g\left(\left[L_1 - \Gamma_1 + C_1(A_1 + P)\right]^+\right) = g\left(\left[L_2 - \Gamma_2 + C_2(A_2 + P)\right]^+\right) \tag{5}$$

(a)

MOTONEURON POOL
ACTIVATION LEVEL

BIG CELL
ZONE

RECRUITMENT THRESHOLD

SMALL CELL
ZONE A_1 A_2

(b)

BIG CELL
ZONE

RECRUITMENT THRESHOLD
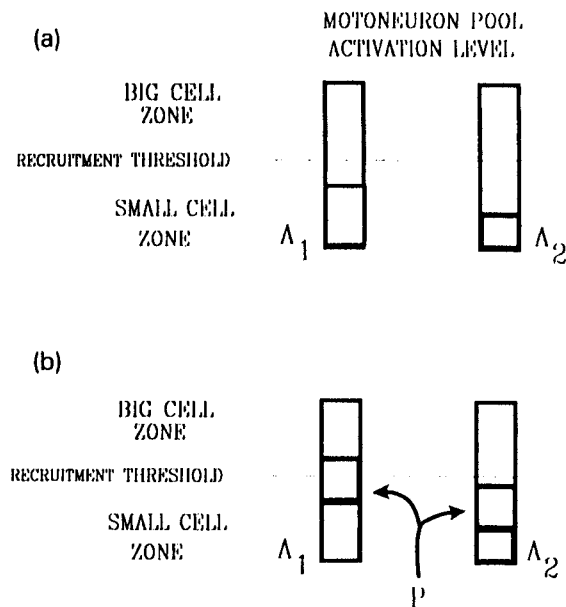
SMALL CELL
ZONE A_1 A_2

P

Fig. 8. When opponent motoneuron populations obey the size principle, a co-contractive signal P sent in parallel to both populations can disrupt the joint position code. (a) Signals A_1 and A_2 supraliminally activate only small cells in opposing channels and their relative sizes determine the balance of muscular forces and thus the equilibrium joint position. (b) With $A_1 > A_2$, co-contractive signal P causes the total input $A_1 + P$ to exceed the big cell threshold while input $A_2 + P$ remains below the big cell threshold. Thus part of the signal P is subjected to greater amplification in channel 1 than in channel 2. Unless compensated, this would create a new balance of forces and cause an unwanted joint rotation.

for arbitrary P and the same initial values of L_i only if $A_1 = A_2$ (see explanation in fig. 8). Thus a co-contractive input P aimed at stabilizing limb position could instead cause a large limb rotation. This would constitute a failure to factorize length and tension.

In the light of this problem, one might propose that C_i and L_i should interact multiplicatively to produce force. Though this would reduce the problem, the proposal amounts to a claim that the primary effect of changing M_i is a change in the stiffness $(\Delta F / \Delta L)$ of a reflexive (deafferented) muscle. However, experimental data show that stiffness changes relatively little as M_i changes; the primary effect of changing M_i is a change in the threshold length for force development, as suggested in eq. (1) and fig. 7 (Feldman 1986; Rack and Westbury 1969).

If left uncompensated by the spino-muscular system, a *different* pair of signals A_1 and A_2 would have to be learned to specify the *same* joint angle for every distinct value of the nonspecific compliance

control signal, P. We now suggest how the spino-muscular system may compensate for position distortions created by the size principle. It thereby avoids a combinatorial explosion in the learning required for limb stabilization across a wide range of joint compliance settings.

11. Automatic compensation by the Renshaw-IaIN pathway for unequal amplifications of co-contractive signals

Renshaw cells (see fig. 6), which receive efferent copies of motoneuronal outputs as their inputs (Renshaw 1946), are well situated to play a compensatory role. In Bullock and Grossberg (1988d), we hypothesized that opponent Renshaw populations R_1 and R_2 measure the output of their respective alpha-motoneuron populations, $\alpha\text{-}MN_1$, and $\alpha\text{-}MN_2$, and compare those outputs via mutually inhibitory signals (fig. 6; see also Ryall 1970). A consensus emerges regarding which MN channel to inhibit via Renshaw feedback, and which to disinhibit via feedback along the Ia interneuron (IaIN) pathway. Suppose that a co-contractive input, P, to $\alpha\text{-}MN_1$ and $\alpha\text{-}MN_2$ occurs when input A_1 exceeds A_2 and that the activity of $\alpha\text{-}MN_1$ is consequently multiplied by a larger factor than that of $\alpha\text{-}MN_2$ due to the size principle (fig. 8). Then R_1 also becomes much more active due to a size-correlated synaptic weighting on $\alpha\text{-}MN_1$ axon collaterals to R_1 (Cullheim and Kellerth 1978; Pompeiano 1984). Because the opposing R_2 has not experienced as large an input increment, R_1 will transiently become more active than R_2 by an amount that scales with the *difference* between the α-MN output increments due to the change in P. Thus, this system calculates a *predicted error* due to unequal amplifications of co-contractive inputs. This predicted-error signal directly inhibits $\alpha\text{-}MN_1$ and, by inhibiting $IaIN_1$, indirectly activates $\alpha\text{-}MN_2$. Both actions work to zero the error signal, and thereby pre-empt occurrence of an actual rotation error, without negating either the shared increment in $\alpha\text{-}MN_i$ activation required to increase joint stiffness (see fig. 10, below), or the joint angle setting determined by the different descending inputs, A_1 and A_2, to opponent α-MN and IaIN populations (see fig. 9, below).

This conjecture has been supported by our computer simulations, which assumed an elbow-like rotary joint affected by two opponent muscles, each of which is inserted in the moving segment one unit from

the axis of rotation. The distance from muscle origin to the axis of rotation was 20 units, and the midpoint of the limb's 180° excursion was stipulated to be at joint angle $\theta = 0°$. Origin-to-insertion muscle lengths, L_i, were thus functions of θ:

$$L_1 = \sqrt{(\cos \theta)^2 + (20 - \sin \theta)^2}, \qquad L_2 = \sqrt{(\cos \theta)^2 + (20 + \sin \theta)^2}.$$

$$(6)$$

Because these simulations concerned only large-scale effects on equilibrium joint angle, we ignored force-velocity effects and chose a simple linear force law

$$F_i = k[L_i - \Gamma_i + C_i]^+,$$

$$(7)$$

where $k = 0.5$, $\Gamma_i = 20.9$ and $i = 1, 2$. Limb dynamics were governed by equation

$$\frac{d^2}{dt^2}\Theta = \frac{1}{m}\left(F_1 - F_2 - n\frac{d\Theta}{dt}\right),$$

$$(8)$$

where m represents mass and n is a damping coefficient. We use forces rather than torques in (8) to illustrate the compensatory properties of the Renshaw-IaIN network. This network is not able to compensate for the moment-arm variation that creates a discrepancy between the muscle force balance and the torque balance within the opponent system. A learning process capable of providing moment-arm compensation is described in section 15.

Contractile state C_i was governed by (2) with $\Gamma_F = 1$. Variables β_i and B_i were defined by:

$$\beta_i = 0.05 + 0.02(A_i + P), \qquad B_i = 2 + 20(A_i + P).$$

$$(9)$$

Both variables grow as a function of total descending input $A_i + P$ to the MN pools in channel i, but β_i grows with a smaller slope. Use of β_i and B_i in eqs. (2) and (9) approximates α-MN recruitment effects that occur as a result of the size principle.

Recruitment of larger motoneurons causes larger inputs to the Renshaw cells (Pompeiano 1984). In our lumped model, this effect was

absorbed into a single variable, z_i, which increases with recruitment extent, approximated by $A_i + P$. The equations for opponent Renshaw populations were thus

$$\frac{d}{dt} R_i = \phi(\lambda B_i - R_i) z_i M_i - R_i(1 + R_j), \tag{10}$$

$$z_i = 0.2 + 0.8(A_i + P), \tag{11}$$

where $\{i, j\} = \{1,2\}$, $\phi = 0.2$, and $\lambda = 5$. Eq. (10) represents a membrane equation (Hodgkin and Huxley 1952) embedded in a shunting competitive network (Grossberg 1973, 1982).

We modeled the opponent alpha-motoneuron populations via the shunting competitive network

$$\frac{d}{dt} M_i = \phi\left[(\lambda B_i - M_i)(A_i + P + \chi E_i)\right] - M_i(\delta_i + \Omega R_i + \rho F_i + I_j), \tag{12}$$

where $\{i, j\} = \{1,2\}$, $\delta_i = 1, \chi = 0$, $\rho = 0$ or 1, and $\Omega = 0$ or 1. Inhibitory inputs I_j come from the IaINs (fig. 6) and excitatory inputs E_i from the muscle spindles. Inhibitory input ρF_i allowed study of the role of the force feedback known to originate in Golgi tendon organs and to be passed to α-MNs via IbINs. IaIN dynamics were modeled without direct dependence on B_i, and without a co-activating input P:

$$\frac{d}{dt} I_i = \phi(10 - I_i)(A_i + \chi E_i) - I_i(1 + \Omega R_i + I_j). \tag{13}$$

In our simulations, variables A_1, A_2, and P were independent variables and variables L_i, F_i, and θ were dependent variables. Spindle feedback signals E_1 and E_2 in Eqs. (12) and (13) were gated off in our simulations by setting $\chi = 0$. This allowed us to test the ability of the Renshaw-IaIN-MN feedback circuit to achieve position code invariance without assistance from stretch reflexes.

When Renshaw feedback was absent ($\Omega = 0$), changing P while A_1 and A_2 remained fixed led to large rotations. When Renshaw feedback was present ($\Omega = 1$), rotations due to changing P with fixed A_1 and A_2 were small. Generally, when the system was not operating in the
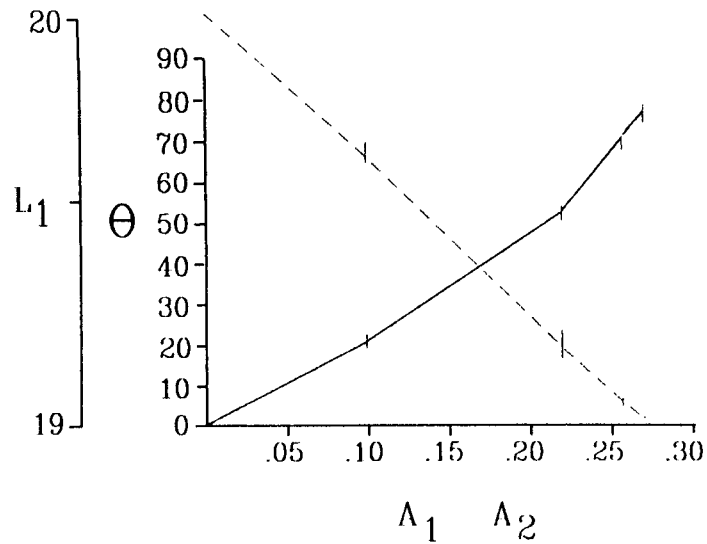
Fig. 9. Summary of simulations demonstrating independent control of length and tension in the FLETE model. Muscle length L_1 (dashed line) is a linear function of $A_1 - A_2$ and varies little despite large changes in co-contractive signal P. Joint angle θ (solid line) is shown for comparison. See text for details.

saturation range, excursions were $< 1°$. On the other hand, the forces F_i, which were monotone increasing in P, varied over a large range. This was the invariance property we sought. Fig. 9 plots L_1 and θ versus $A_1 - A_2$ for half of a full range of limb excursions. The half not shown, for $A_1 - A_2 < 0$, is symmetrical. The small residual effect on position of changing P in the range 0–.8 is shown by the vertical bars,
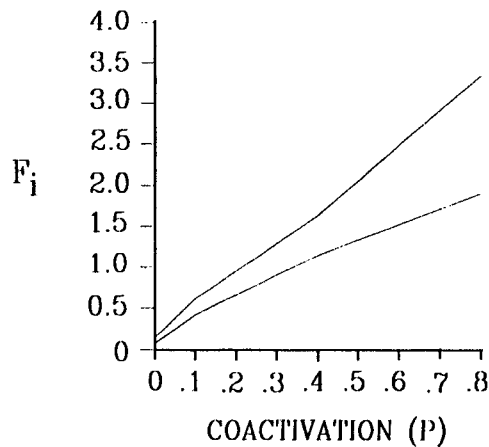

Fig. 10. Force rises more quickly as a function of co-contractive signal P with mutual Renshaw inhibition (upper curve) than without it (lower curve).

which indicate the full range of variation, not standard deviations. Without the force feedback ($\rho = 0$) in (12), the range of variation due to P was slightly larger, but more importantly, the range was no longer centered at the $P = 0$ point. Thus in addition to its ability to help compensate for muscle fatigue (Kirsch and Rymer 1987), it appears that the force feedback from Golgi tendon organs may correct a mean bias introduced by the size principle.

Fig. 10 illustrates the importance of including mutual inhibition, via term $-R_i R_j$ in (10), between opponent Renshaw cell populations. Without it, increments in P produce diminishing returns of force output from each muscle in the system. With it, force development is approximately linear in P. Compatible results regarding only α-MN, Renshaw cell interactions may be found in a one-muscle-channel simulation study of force output by Akazawa (1989).

12. Evidence for assumed distribution of Renshaw connectivity

Two critical hypotheses of our model are (a) that Renshaw cells participate in the size principle and (b) that the computational unit is the pair of opponent muscle channels.

A variety of evidence supports the hypothesis that Renshaw cells participate in the size principle. In our simulations, this assumption was implemented by scaling up Renshaw population parameters in parallel with motor-unit rescaling as $A_i + P$ grows. Recent experiments surveyed by Pompeiano (1984) concur that 'recurrent inhibition is produced mainly by large phasic neurons that are recruited late' (p. 526). In particular, Pompeiano and Wand (1976; Wand and Pompeiano 1979) produced functional evidence for such a size-dependency, and Cullheim and Kellerth (1978) produced convergent anatomical evidence by showing that larger, phasic motoneurons make many more synaptic contacts with Renshaw cells than smaller, tonic motoneurons.

The second hypothesis has been well supported since Sherrington's (1906) observations of reciprocal inhibition, but is oddly ignored in many treatments. Our treatment extends the reciprocal inhibition principle, which is a 'biggest competitor wins' principle at the IaIN stage (fig. 6), by including Renshaw populations which compete before supplying inhibitory feedback to the model's IaINs and alpha-

motoneurons (Miller and Scott 1977; Pompeiano 1984). Because the channel with the larger Renshaw activity receives more inhibition, reciprocal inhibition at the Renshaw stage follows a 'biggest competitor loses' principle. This property extends the classical role of the Renshaws in stabilizing the peripheral skeleto-motor system; Renshaw inhibition works against extreme joint angle excursions and complements the intrinsic damping characteristics of muscles.

More generally (fig. 6), the FLETE model assumes that Renshaw cells have an inhibitory effect at three sites. The recurrent inhibition to the alpha-motoneuron population that excites them has long been well known (Renshaw 1941; Eccles et al. 1954; see Pompeiano 1984, for recent review). Inhibition of the IaIN population in the same outflow channel was demonstrated by Hultborn et al. (1971) and confirmed by others (see Pompeiano 1984: 512–513). Renshaw inhibition of the Renshaw population of the opposing muscle channel, suspected since Renshaw (1946), has been convincingly demonstrated by Ryall (1970). Though there is also evidence that Renshaws have an inhibitory effect on gamma motoneurons (Pompeiano 1984: 509–511), the effect is known to be attenuated relative to that on alpha-MNs. Though nearly all alpha-MNs are inhibited by Renshaws, only about half of gamma-MNs are so inhibited, and in lesser degree.

The model also assumes that Renshaw cells are directly affected by an excitatory input from the alpha-motoneurons (see Renshaw 1941), and an inhibitory input from the opposing-channel's Renshaw cells (noted above). A Renshaw inhibiting, α-MN exciting stretch feedback from spindle organs via group II fibers (Fromm et al. 1977), is fully consistent with FLETE and will be incorporated in future simulations. In this connection, we note that a descending inhibitory input from the red nucleus to Renshaw populations is also well documented (Henatsch et al. 1986). This inhibitory red nucleus output is coupled with another rubral output that excites alpha-motoneurons in the same outflow channel. Thus this descending rubral signal is analogous to the inflowing type II spindle signal. If this parallel rubral output is a reciprocal command (always increasing in one channel while decreasing in the opposing channel), it can be seen to be part of a feedforward adaptive gain control system (Grossberg and Kuperstein 1986, 1989), which gradually learns to supply *predictively* the compensations the peripheral circuit can only supply *reactively* (see section 15).

13. Prior proposals regarding Renshaw function

Proposals regarding Renshaw function have evolved rapidly in recent years. Shepherd (1979) acknowledged that their function remained mysterious despite the long-standing hypothesis that they might serve as a source of surround inhibition (and thus perhaps to contrast enhance the motor-output signal). In the same year Hultborn et al. (1979) proposed that the Renshaws were well situated to control the gain of the alpha-motoneuron pool's response to excitatory inputs. This proposal was often restated in terms of controlling the gain of the stretch reflex (e.g., McMahon 1984), a picture since reinforced by discovery of the descending (rubrospinal) pathways that both inhibit Renshaw cell activity (thus disinhibiting alpha-motoneurons) and excite alpha-motoneurons, resulting in a higher-gain stretch reflex (Henatsch et al. 1986) among other effects. The common scenario imagined for such Renshaw modulation was during muscle contraction intended to produce movement. This proposal is not in conflict with the present proposal, in which muscle co-contraction intended to prevent movement requires that the Renshaw pathway not be inhibited by descending signals.

A model by Miller and Scott (1977) shares our emphasis on competition between opponent Renshaw populations. However, the authors assumed that such competition implicated the Renshaw-IaIN pathway in locomotor pattern generation, a different function than the one here proposed. Subsequent research (Pratt and Jordan 1987) appears to have ruled out the possibility that the Renshaw-IaIN pathway is part of a spinal locomotor generator, but we believe Miller and Scott (1977) were correct to implicate the pathway in burst pattern generation as such (see section 18).

Finally, though some aspects of our model are similar to Feldman's (1986) well-known 'λ' model of skeleto-motor control, neither of our decending control signals, A_i and P, correspond to Feldman's stretch-reflex parameter λ. Moreover, we believe that continued use of lumped parameters like λ, and a kindred overemphasis on the concept of stretch reflex, may hinder attempts to understand how the neuromuscular system is parsed into functional subsystems. A case in point is the discovery, upon unlumping reciprocal and co-contractive inputs, that the Renshaw-IaIN pathway may play a role far more interesting than being an epicycle of the stretch reflex.

14. Physiological evidence for separate cortical control of non-selective co-contractive input to motoneurons

FLETE model simulations of Renshaw function were based on the assumption that the co-contractive signal, P, is sent in parallel to small and large MNs alike in both outflow channels (fig. 8). This hypothesis is supported by data of Humphrey and Reed (1983), who subjected monkeys to high-frequency, alternating-direction, torque perturbations at the wrist joint after they trained the monkeys to actively maintain their wrist angle within a small angular tolerance zone. To prevent the imposed torques from rotating their wrists to angles outside the desired range, monkeys instated high levels of tonic co-contraction in wrist flexors and extensors. Measurements of motor unit activity showed that high levels of co-contraction were achieved non-selectively and in accord with the size principle. In particular, Humphrey and Reed (1983) concluded that 'As the speed of joint perturbation rises, the modulated [reciprocal] input to the MN pools is increased and a tonic coactivation signal is added. ... Thus, an explanation of our observed MN firing patterns requires no assumption of selectivity of descending inputs to motor units of different type, nor of any recruitment order different from that established in previous studies .... Both [reciprocal and co-activating] control signals appear to converge on both fast and slow-twitch MNs' (p. 366).

Humphrey and Reed (1983) were also able to identify a central source of co-activation signals. In section 5, we cited evidence from Georgopoulos that precentral motor cortex (Area 4) served as a site of VITE-like DV computations and thus as a source of reciprocal commands received by spinal motor centers. Whereas Humphrey and Reed (1983) observed similar reciprocally-engaged precentral cells, they also discovered a new class of tonically active neurons they called S^{Δ}; cells (S = steady, Δ = shift). These neurons, also found in precentral Area 4, predominated in a zone slightly anterior to the DV-like cells, and 'when the animal voluntarily co-contracted his wrist muscles, as in stabilization of the wrist or tightening of a grip on the handle, these cells discharged in a brisk and tonic manner' (Humphrey and Reed 1983: p. 363). Moreover, microstimulation (12 to 20 μA) in the anterior, S^{Δ} cell, zone evoked a co-activation of flexor and extensor muscles at the wrist and in some cases at other arm joints. Thus the primary motor cortex seems to be a source of both the specific (reciprocal) and

the non-specific (co-contractive) signals assumed to ultimately converge on the spinal motoneurons in the FLETE model.

15. Learned cerebellar compensation for variable moment-arms using spindle organ error signals

One additional intrinsic source of variability remains to be addressed. As noted in section 2, joint rotations depend on muscle torques rather than muscle forces as such. Thus eq. (8) must be replaced by equations

$$\frac{d^2}{dt^2}\theta = \frac{1}{m}\left(T_1 - T_2 + T_e - n\frac{d\theta}{dt}\right) \tag{14}$$

and

$$T_i = D_i F_i, \qquad i = 1, 2. \tag{15}$$

D_i is the moment-arm of force F_i, T_i is the torque associated with muscle i, and T_e is an external torque (see next section). The moment-arm is the perpendicular distance between the line of action of F_i and the axis of joint rotation. Eq. (15) says that the torques T_i are a function of both the forces F_i and the moment-arms D_i. The latter are in turn functions of joint angle θ:

$$D_1 = \frac{20}{\sqrt{\left(\dfrac{\sin\theta - 20}{\cos\theta}\right)^2 + 1}}, \tag{16}$$

$$D_2 = \frac{20}{\sqrt{\left(\dfrac{\sin\theta + 20}{\cos\theta}\right)^2 + 1}}. \tag{17}$$

Variables D_i introduce yet another threat to position-code invariance. However, because of the factorization properties already described, moment-arm compensation may take an especially simple form in a system based on the FLETE module. Recent simulations show that
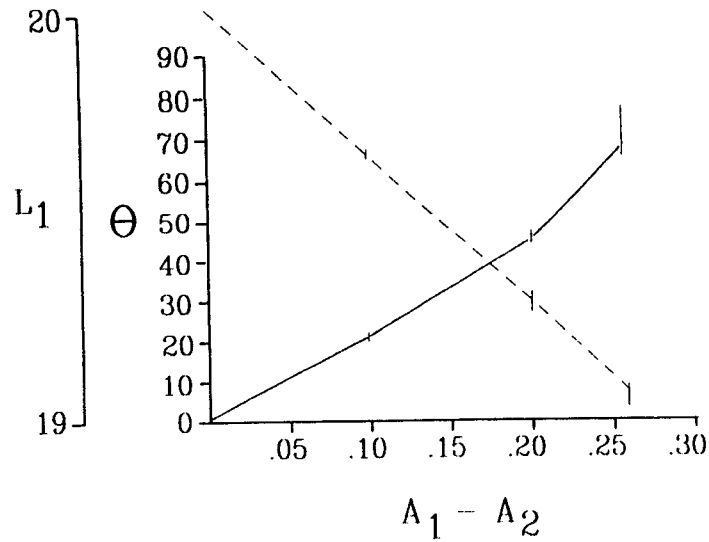
Fig. 11. Immediate reactive compensations and long-term adaptation of coefficients in feedforward signal pathways, both mediated by spindle-organ feedback signals, allow the FLETE model to ensure independent control of muscle length and tension despite angle-dependent variations in muscle mechanical advantage. See text and fig. 9 for details.

adaptive gains $g(A_1, A_2)$ may be learned by mechanisms schematized in panels 10 and 8 of fig. 1 (see also Ito 1984: 328) and applied with opposite sign to alter the coefficients of total descending signals, $A_i + P$, to the opponent alpha motoneuron populations. In particular, the new descending signals become:

$$S_1 = [1 - g(A_1, A_2)](A_1 + P),\tag{18}$$

$$S_2 = [1 + g(A_1, A_2)](A_2 + P).\tag{19}$$

In our theory the adaptive gains $g(A_1, A_2)$ in eqs. (18) and (19) are learned with the aid of collateral ascending projections that arise from muscle spindle organs. These pathways carry muscle-length error signals (see fig. 1, panel 10). In eqs. (12) and (13), these error signals cause fast reactive corrections in motoneuron activation via the inputs E_i. Here we assume that they also cause slower adaptive corrections via a learning process which affords predictive elimination of positional errors on future performance trials. In particular, the muscle-length error signals change the adaptive gains $g(A_1, A_2)$ in such a way that the spindle error signals eventually approach zero. This learning process is assumed to occur in the cerebellum. When the learned gains

$g(A_1, A_2)$ are used to bias the descending signals $A_i + P$ in eq. (12), and $\chi = 1$ in eqs. (12) and (13), then moment-arm effects are compensated and position-code invariance is restored, as shown in fig. 11.

Each activation pattern (A_1, A_2) of descending opponent commands is assumed to control a different adaptive gain $g(A_1, A_2)$. Grossberg and Kuperstein (1986, 1989) have shown how such descending commands (A_1, A_2) can give rise to parallel pathways, or corollary discharges, that are transformed further by a competitive learning network. Using this scheme, different activation patterns (A_1, A_2) can be converted into different locations in a spatial map, which can, in turn, activate different pathways, each of which can learn a distinct adaptive gain. In such a scheme, not every activation pattern (A_1, A_2) can control its own private gain-control pathway, since infinitely many patterns but only finitely many pathways exist. Nonetheless, a coarse coding is learned whereby sufficiently different activation patterns can activate different gain-control pathways.

The learning rule that was used started with zero initial gains $g(A_1, A_2)$. For patterns (A_1, A_2) learning caused $g(A_1, A_2)$ to increase if $E_2 > E_1$ and to decrease if $E_1 > E_2$. In particular,

$$\frac{\mathrm{d}}{\mathrm{d}t} g(A_1, A_2) = \epsilon(E_2 - E_1).\tag{20}$$

Here the magnitude of ϵ controls learning rate. This adaptive gain control process used an opponent organization in two different senses. First, the error signals E_1 and E_2 change the gains g via an opponent
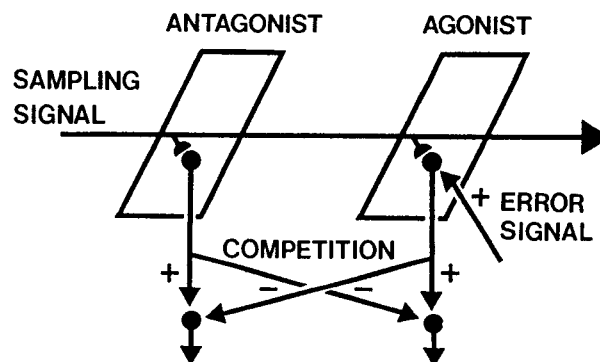

Fig. 12. One possible design allowing opponent modifications of adaptive gains in a simplified cerebellar model. Reprinted with permission from Grossberg and Kuperstein (1986, 1989), chapter 3.

error term $E_2 - E_1$. Second, the gains g have an opponent effect, via terms $(1 - g)$ and $(1 + g)$ in (18) and (19), upon the output signals of the opponent movement channels. Such an opponent organization is reminiscent of the opponent action of Renshaw feedback at the spinal level: the net signal emerging from the Renshaw stage competition between opponent channels simultaneously decrements one channels' output and increments the opposing channel's output. Grossberg and Kuperstein (1986, 1989) seem to have been the first to use opponent learning and output organization of adaptive gains during sensory-motor control. They suggested that such an opponent organization may explain the fractured somatotopy of the cerebellum. Fractured somatotopy occurs when internal representations of sensory or motor sites that are non-adjacent in the body are nonetheless juxtaposed in the cerebellum. As schematized in fig. 12, juxtaposition of cerebellar strips responsible for controlling somatotopically non-adjacent but physically opponent muscles provides a simple device for ensuring such an opponent learning and performance scheme.

The strategy of skill development discussed in section 1 – starting with high co-contraction and low speed – is a good method for rapidly learning moment-arm correction gains g. Because these gains are independent of the compliance control signal P, the factorization property that gives the FLETE model its name is preserved.

16. Co-contractive and stretch feedback control of compensation for external torques

To run the simulations summarized in fig. 11, we used a simple model of the subsystem composed of γ-MNs, intrafusal muscles, and spindle organs. Our model includes those aspects needed to test factorization of position and compliance at equilibrium. A subsequent paper will analyse transients during movement (Bullock and Grossberg, in press). We modeled γ-MN activity N_i by

$$\frac{\mathrm{d}}{\mathrm{d}t} N_i = \phi\left[(10 - N_i)A_i\right] - N_i(1 + A_j),$$ (21)

intrafusal muscle contraction U_i by

$$\frac{\mathrm{d}}{\mathrm{d}t} U_i = 4N_i - U_i,$$ (22)

and spindle organ response via

$$\frac{d}{dt} W_i = [U_i + L_i - \Gamma_i]^+ - W_i. \tag{23}$$

Eq. (21) embodies the ideas that the γ-MNs do not participate in the size principle – unlike the α-MNs in (12) –, do not receive a co-contractive input P, and that the effect of inputs A_1 and A_2 is normalized by the shunting term $- N_i(1 + A_j)$. Eq. (22) says that the intrafusal muscle contraction U_i is proportional to the γ-MN activation level N_i. Eq. (23) says that the spindle organ responds to intrafusal muscle contraction U_i and extrafusal muscle stretch $L_i - \Gamma_i$. In addition, χ in eq. (12) was set equal to 1 and E_i was defined by

$$E_i = W_i. \tag{24}$$

Because χE_i was non-zero in these simulations, we replaced eq. (9) by

$$\beta_i = 0.05 + 0.02(S_i + \chi E_i), \qquad B_i = 2 + 20(S_i + \chi E_i), \tag{25}$$

with S_1 and S_2 defined by (18) and (19), to assure that stretch feedback E_i played a role in rescaling parameters of active motor units, as occurs *in vivo* (Humphrey and Reed 1983). Because a nonlinear force law also contributes, we replaced the linear law in (7) by

$$F_i = k\left([L_i - \Gamma_i + C_i]^+\right)^2. \tag{26}$$

Although it made little difference in model performance, for greater realism we replaced the linear force feedback term ρF_i in (12) with ρX_i, where X_i models the potential of the ith IbIN population. Variable X_i obeys the membrane equation

$$\frac{d}{dt} X_i = \phi[(10 - X_i)F_i] - X_i. \tag{27}$$

Compliance control by this model is summarized in fig. 13, which shows that the angular displacement $\Delta\theta$ induced by an external torque T_e applied to the model arm varies inversely with P. This shows that increases in co-contractive signal P reduce arm compliance in the FLETE model. Full load compensation is not achieved for any P value
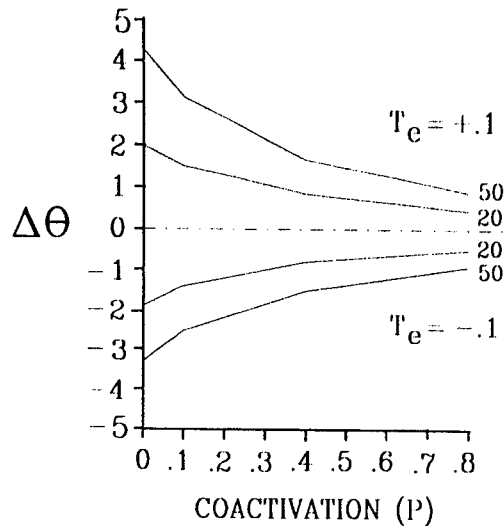
Fig. 13. A demonstration of compliance control in the FLETE model. Angular displacements $\Delta\theta$ caused by imposed torques $T_e = 0.1$ and $T_e = -0.1$ are decreasing functions of co-contractive signal P. Starting θs were 20° and 50°.

because the stretch reflex feedback gain of the network as a whole was less than unity.

The simulations summarized in fig. 13 were run with $\delta_i = 0$ in (12). Then the model α-MNs behave as neural integrators. With $\delta_i = 1$, as in previous simulations, leaky integrator behavior was modeled. Both parameter choices are consistent with the observation that α-MNs exhibit plateau potentials *in vivo* (Hounsgaard et al. 1986).

17. Interplay of fast automatic reactive control and slow adaptive predictive control: a new synthesis

The endpoint of the present construction – the use of length-error feedback for load compensation – has traditionally been a starting point for analyzing the spino-muscular system. In the traditional story (Merton 1953), muscle length was assumed to be a controlled variable, and the spindle organs measured length errors to trigger fast automatic reactive compensations for deviations from desired length.

Some reactive compensation is indeed provided by the classical stretch reflex constituted by the spindle → α-MN → muscle pathway (fig. 6). Continuous reactive feedback compensations must, however, be kept small relative to the measured deviation in order to avoid instabili-

ties such as persistent tremor (Rack 1981). Thus continuous reactive compensation via the stretch reflex can provide only partial compensation.

While we also believe that muscle length is a controlled variable, our explanation of how length can be precisely controlled is different than that imagined by Merton (1953) or more contemporary workers. In our account, length-error feedback does both less and more than other scientists have described. It does less because fast automatic compensation for threats to length control is also provided to a significant degree by the Renshaw-IaIN subsystem (section 11). It does more by directing slow learning of adaptive gains to predictively control movement commands (section 15). Such slow adaptive adjustment of feedforward signals to the α-MNs allows nearly complete pre-emptive compensation for predictable sources of deviation from desired length, without creating instabilities. (See Hasan and Enoka (1985) for discussion of why compensation can only be nearly complete.) By conceiving of the length-error feedback in this teaching role in addition to its stretch-reflex role, and by deferring its consideration until other potential spinal resources for length-error compensation were thoroughly explored, we have been able to construct a theory of how position-code invariance may be achieved by the spino-muscular system that sheds new light on features of its circuitry that have been anatomically well-known but functionally mysterious for a long time.

18. Compatibility of the FLETE model with other properties of the spino-muscular system

Many other properties of the spino-muscular system are clarified by the theoretical perspective adopted in this paper. Three classes of phenomena to be systematically treated in forthcoming papers of this series are: (1) muscle operating characteristics; (2) neuronal and muscular transients generated during transitions between equilibrium states of the system; and (3) additional spinal and supraspinal connectivities. Here a few remarks must suffice (see also Bullock and Grossberg 1989). Muscle operating characteristics aid position-code invariance during movement and posture. For example, the force-velocity relation for muscle (Hill 1938) assists damping during shortening contractions, and the asymmetrical, non-monotonic force–length relation (Gordon et al.

1966) provides some moment-arm compensation. Computer simulations indicate that a rapid, reciprocal, ramp-like change in A_1 and A_2 causes the FLETE circuit to transiently generate tri-phasic burst patterns involving agonist and then antagonist (Bullock and Grossberg, in press). Though the origin and adaptive tuning of such bursts is a complex issue, this finding partially corroborates Feldman's (1986) prediction that the spino-muscular system would prove capable of generating such bursts, which are frequently observed *in vivo* (Lestienne 1979).

Finally, many additional aspects of known connectivity may be incorporated into a composite VITE–FLETE-Cerebellum model. For example, the inhibitory feedback from spindle II fibers to Renshaw cells (Fromm et al. 1977), and the descending projections from red nucleus to Renshaw cells (Henatsch et al. 1986) can be interpreted in terms of balancing reactive and predictive contributions to position-code invariance, because the red nucleus lies in the pathway from cerebellum to spinal cord.

19. Nonspecific signals and the development of voluntary control

The present article provides two examples of how to understand a key paradox in the organization of voluntary motor control. When we exercise voluntary control, or acts of 'will', it seems that we do something quite simple, yet we know that such control involves the coordinated activity of millions of neural and muscular units. One device whereby voluntary control is simplified is the use of *nonspecific* control signals. A nonspecific signal is a scalar signal that is generated at a single command source and broadcast, through a parallel fan-out of pathways, to many target cells. It is then up to the target cells to react appropriately to the widely broadcast signal. If each cell reacts in a state-dependent manner, a nonspecific signal can exert voluntary control over an entire array of events without requiring conscious knowledge of the controlled array.

In the VITE circuit, a single GO signal sent in parallel to a large number of primed muscle-control channels can initiate a goal-oriented synchronous movement trajectory, and control its speed without disrupting its form. In the FLETE circuit, a single co-contraction signal sent in parallel to a large number of muscle channels can control joint

rigidity without disrupting postural stability. Both circuits thus clarify the old mystery about volitional action: if every act is so complex, why do volitional acts, or acts of 'will', seem to be so simple?

Once such invariance-preserving components evolve, they can be expected to be incorporated into many subsequent evolutionary specializations (Bullock 1987; Grossberg and Kuperstein 1986, 1989; Lieberman 1984; Powers 1973; Simon 1969). Here and elsewhere, we have argued that the VITE architecture or close variants may have been replicated across many systems which control phasic goal-oriented movements, including both arm and speech movements (Bullock and Grossberg 1988a, 1988b), and the circuit of fig. 6, which is mathematized in the FLETE model, is known to exist throughout the higher vertebrates. Similarly, the cerebellum serves as an adaptive gain control stage in a wide range of motor systems (Grossberg and Kuperstein 1986, 1989; Ito 1984; Kawato et al. 1987). Despite initial appearances of overwhelming complexity, perhaps we may reasonably hope that the discovery of a modest number of robust and broadly applicable circuits will allow us to explain a large portion of the basic motor competence of higher vertebrate species.

References

Abbs, J.H., V.L. Gracco and K.J. Cole, 1984. Control of multi-movement coordination: Sensori-motor mechanisms in speech motor control. Journal of Motor Behavior 16, 195–231.

Akazawa, K., K. Kato and K. Fujii, 1989. A neural network model of force control based on the size principle of motor unit. Proceedings of the International Joint Conference on Neural Networks 1. pp. 739–746.

Albus, J.S., 1971. A theory of cerebellar function. Mathematical Biosciences 10, 25–61.

Anderson, M.E. and F.B. Horak, 1985. Influence of the globus pallidus on arm movements in monkeys. III. Timing of movement-related information. Journal of Neurophysiology 54, 433–448.

Bedford, F., 1989. Constraints on learning new mappings between perceptual dimensions. Journal of Experimental Psychology: Human Perception and Performance 15, 232–248.

Beggs, W.D.A. and C.I. Howarth, 1972. The movement of the hand towards a target. Quarterly Journal of Experimental Psychology 24, 448–453.

Bernstein, N., 1967. The coordination and regulation of movements. New York: Pergamon Press.

Bizzi, E., N. Accornero, W. Chapple and N. Hogan, 1984. Posture control and trajectory formation during arm movement. Journal of Neuroscience 4(11), 2738–2744.

Bullock, D., 1987. 'Socializing the theory of intellectual development'. In: M. Chapman and R.A. Dixon (eds.), Meaning and the growth of understanding: Wittgenstein's significance for developmental psychology. New York: Springer-Verlag. pp. 187–218.

Bullock, D., G.A. Carpenter and S. Grossberg, 1991. 'Self-organizing neural network architectures for adaptive pattern recognition and robotics'. In: V. Milutinovic and P. Antognetti (eds.), Neural networks and their applications. Englewood Cliffs, NJ: Prentice Hall. pp. 33–53.

Bullock, D. and S. Grossberg, 1986. Neural dynamics of planned arm movements: Synergies, invariants, and trajectory formation. Paper presented at the symposium on Neural Models of Sensory-Motor Control at the annual meeting of the Society for Mathematical Psychology, Cambridge, MA, August 20.

Bullock, D. and S. Grossberg, 1988a. Neural dynamics of planned arm movements: Emergent invariants and speed-accuracy properties during trajectory formation. Psychological Review 95(1), 49–90.

Bullock, D. and S. Grossberg, 1988b. 'The VITE model: A neural command circuit for generating arm and articulator trajectories'. In: J.A.S. Kelso, A.J. Mandel, and M.F. Shlesinger (eds.), Dynamic patterns in complex systems. Singapore: World Scientific. pp. 305–326.

Bullock, D. and S. Grossberg, 1988c. 'Self-organizing neural architectures for eye movements, arm movements, and eye-arm coordination'. In: H. Haken (ed.), Neural and synergetic computers. Berlin: Springer-Verlag. pp. 197–228.

Bullock, D. and S. Grossberg, 1988d. Neuromuscular realization of planned trajectories. Neural Networks 1, Supplement 1, 329.

Bullock, D. and S. Grossberg, 1989. 'VITE and FLETE: Neural modules for trajectory formation and postural control'. In: W.A. Hershberger (ed.), Volitional action. Amsterdam: North-Holland. pp. 253–297.

Bullock, D. and S. Grossberg, in press. Emergence of tri-phasic muscle activation from the nonlinear interactions of central and spinal neural network circuits. Human Movement Science.

Cooke, J.D., 1980. 'The organization of simple, skilled movements'. In: G.E. Stelmach and J. Requin (eds.), Tutorials in motor behavior. Amsterdam: North-Holland. pp. 199–212.

Cooke, J.D. and V.A. Diggles, 1984. Rapid error correction during human arm movements: Evidence for central monitoring. Journal of Motor Behavior 16, 348–363.

Cullheim, S. and J.O. Kellerth, 1978. A morphological study of the axons and recurrent axon collaterals of cat α-motoneurones supplying different functional types of muscle unit. Journal of Physiology (London) 281, 301–313.

DeJong, R., M.G.H. Coles, G.D. Logan and G. Gratton, 1990. In search of the point of no return: The control of response processes. Journal of Experimental Psychology: Human Perception and Performance 16, 164–182.

Ebner, T., 1989. Representation of movement kinematics and accuracy in the premotor cortex. Paper presented at the symposium on System Solutions to Motor Problems, Tempe, Arizona, 27–29 October.

Eccles, J.C., P. Fatt and K. Koketsu, 1954. Cholinergic and inhibitory synapses in a pathway from motor-axon collaterals to motoneurones. Journal of Physiology (London) 126, 524–562.

Evarts, E.V. and J. Tanji, 1974. Gating of motor cortex reflexes by prior instruction. Brain Research 71, 479–494.

Feldman, A.G., 1986. Once more on the equilibrium-point hypothesis (λ model) for motor control. Journal of Motor Behavior 18, 17–54.

Fischer, K.W., 1980. A theory of cognitive development: The control and construction of hierarchies of skills. Psychological Review 87, 477–531.

Fisk, J.D. and M.A. Goodale, 1988. The effects of unilateral brain damage on visually guided reaching: hemispheric differences in the nature of the deficit. Experimental Brain Research 72, 425–435.

Fitts, P.M., 1954. The information capacity of the human motor system in controlling the amplitude of movement. Journal of Experimental Psychology 47, 381–391.

Freund, H.-J. and H.J. Büdingen, 1978. The relationship between speed and amplitude of the fastest voluntary contractions of human arm muscles. Experimental Brain Research 31, 1–12.

Fromm, C., J. Haase and E. Wolf, 1977. Depression of the recurrent inhibition of extensor motoneurones by the action of group II afferents. Brain Research 120, 459–468.

Gachoud, J.P., P. Mounoud, C.A. Havert and P. Viviani, 1983. Motor strategies in lifting movements: A comparison of adult and child performance. Journal of Motor Behavior 15, 202–216.

Gahery, Y. and J. Massion, 1985. 'Co-ordination between posture and movement'. In: E.V. Evarts, S.P. Wise, and D. Bousfield (eds.), The motor system in neurobiology. Amsterdam: Elsevier. pp. 121–125.

Gaudiano, P. and S. Grossberg, 1990. 'A self-regulating generator of sample-and-hold random training vectors'. In: Proceedings of the International Joint Conference on Neural Networks, Washington, DC. Hillsdale, NJ: Erlbaum.

Gaudiano, P. and S. Grossberg, 1991. Vector associative maps: Unsupervised real-time error-based learning and control of movement trajectories. Neural Networks (in press).

Gaudiano, P. and S. Grossberg, in press. Adaptive vector integration to endpoint: Self-organizing neural circuits for control of planned movement trajectories. Human Movement Science.

Georgopoulos, A.P., J.F. Kalaska and J.T. Massey, 1981. Spatial trajectories and reaction times of aimed movements: Effects of practice, uncertainty, and change in target location. Journal of Neurophysiology 46, 725–743.

Georgopoulos, A.P., J.F. Kalaska, R. Caminiti and J.T. Massey, 1984a. On the relations between the direction of two-dimensional arm movements and cell discharge in primate motor cortex. Journal of Neuroscience 2(11), 1527–1537.

Georgopoulos, A.P., J.F. Kalaska, R. Caminiti and J.T. Massey, 1984b. 'The representation of movement direction in the motor cortex: Single cell and population studies'. In: G.M. Edelman, W.E. Gall, and W.M. Cowan (eds.), Dynamic aspects of neocortical function. New York: Wiley. pp. 501–524.

Goodale, M.A., D. Pelisson and C. Prablanc, 1986. Large adjustments in visually guided reaching do not depend on vision of the hand or perception of target displacement. Nature 320, 748–750.

Gordon, A.M., A.F. Huxley and F.J. Julian, 1966. The variation in isometric tension with sarcomere length in vertebrate muscle fibers. Journal of Physiology 184, 170–192.

Gordon, J. and C. Ghez, 1987. Trajectory control in targeted force impulses, III: Compensatory adjustments for initial errors. Experimental Brain Research 67, 253–269.

Grossberg, S., 1969. On learning of spatiotemporal patterns by networks with ordered sensory and motor components, I. Excitatory components of the cerebellum. Studies in Applied Mathematics 48, 105–132.

Grossberg, S., 1970. Neural pattern discrimination. Journal of Theoretical Biology 27, 291–337.

Grossberg, S., 1973. Contour enhancement, short-term memory, and constancies in reverberating neural networks. Studies in Applied Mathematics 52, 217–257.

Grossberg, S., 1978. 'A theory of human memory: Self-organization and performance of sensory-motor codes, maps, and plans'. In: R. Rosen and F. Snell (eds.), Progress in theoretical biology, Vol. 5. New York: Academic Press. pp. 233–374.

Grossberg, S., 1982. Studies of mind and brain: Neural principles of learning, perception, development, cognition, and motor control. Boston, MA: Reidel Press.

Grossberg, S. and M. Kuperstein, 1986. Neural dynamics of adaptive sensory-motor control: Ballistic eye movements. Amsterdam: Elsevier.

Grossberg, S. and M. Kuperstein, 1989. Neural dynamics of adaptive sensory-motor control: Expanded edition. New York: Pergamon Press.

Hasan, Z. and R.M. Enoka, 1985. Isometric torque-angle relationship and movement-related

activity of human elbow flexors: Implications for the equilibrium-point hypothesis. Experimental Brain Research 59, 441–450.

Henatsch, H.D., J. Meyer-Lohmann, U. Windhorst and J. Schmidt, 1986. Differential effects of stimulation of the cat's red nucleus on lumbar alpha motoneurons and their Renshaw cells. Experimental Brain Research 62, 161–174.

Henneman, E., 1957. Relation between size of neurons and their susceptibility to discharge. Science 26, 1345–1347.

Henneman, E., 1985. The size-principle: A deterministic output emerges from a set of probabilistic connections. Journal of Experimental Biology 115, 105–112.

Hill, A.V., 1938. The heat of shortening and the dynamic constants of muscle. Proceedings of the Royal Society, B 126, 136–195.

Hodgkin, A.L. and A.F. Huxley, 1952 A quantitative description of membrane current and its applications to conduction and excitation in nerve. Journal of Physiology 117, 500–544.

Hogan, N., 1984. An organizing principle for a class of voluntary movements. Journal of Neuroscience 4(11), 2745–2754.

Hollerbach, J.M., S.P. Moore and C.G. Atkeson, 1986. 'Workspace effect in arm movement kinematics derived by joint interpolation'. In: G. Gantchev, B. Dimitrov and P. Gatev (eds.), Motor control. New York: Plenum Press.

Horak, F.B. and M.E. Anderson, 1984a. Influence of globus pallidus on arm movements in monkeys, I. Effects of kainic acid-induced lesions. Journal of Neurophysiology 52, 290–304.

Horak, F.B. and M.E. Anderson, 1984b. Influence of globus pallidus on arm movements in monkeys, II. Effects of stimulation. Journal of Neurophysiology 52, 305–322.

Hore, J., 1987. Loss of set-dependent reactions during cerebellar dysfunction causes limb instability. In: S.P. Wise (ed.), Higher brain functions. New York: Wiley.

Houk, J.C. and W.Z. Rymer, 1981. 'Neural control of muscle length and tension'. In: Handbook of physiology: The nervous system II. Bethesda, MD: American Physiological Society. pp. 257–322.

Hounsgaard, J., H. Hultborn and O. Kiehn, 1986. Transmitter-controlled properties of α-motoneurones causing long-lasting motor discharge to brief excitatory inputs. Progress in Brain Research 64, 39–50.

Hultborn, H., E. Jankowska and S. Lindström, 1971. Relative contribution from different nerves to recurrent depression of Ia IPSPs in motoneurones. Journal of Physiology (London) 215, 637–664.

Hultborn, H., S. Lindström and H. Wigström, 1979. On the function of recurrent inhibition in the spinal cord. Experimental Brain Research 37, 399–403.

Humphrey, D.R., and D.J. Reed, 1983. 'Separate cortical systems for control of joint movement and joint stiffness: Reciprocal activation and coactivation of antagonist muscles'. In: J.E. Desmedt (ed.), Motor control mechanisms in health and disease. New York: Raven Press, pp. 347–372.

Ito, M., 1984. The cerebellum and neural control. New York: Raven Press.

Kawato, M., K. Furukawa and R. Suzuki, 1987. A hierarchical neural-network model for control and learning of voluntary movement. Biological Cybernetics 57, 169–185.

Kirsch, R.F. and W.Z. Rymer, 1987. Neural compensation for muscular fatigue: Evidence for significant force regulation in man. Journal of Neurophysiology 57, 1893–1910.

Kuperstein, M., 1988. Neural network model for adaptive hand–eye coordination for single postures. Science 239, 1308–1311.

Lestienne, F., 1979. Effects of inertial load and velocity on the braking process of voluntary limb movements. Experimental Brain Research 35, 407–418.

Lieberman, P., 1984. The biology and evolution of language. Cambridge, MA: Harvard University Press.

Marr, D., 1969. A theory of cerebellar cortex. Journal of Physiology (London) 202, 437–470.

Mateer, C., 1978. Asymmetric effects of thalamic stimulation on rate of speech. Neuropsychologia 16, 497–499.

McMahon, T.A., 1984. Muscles, reflexes, and locomotion. Princeton, NJ: Princeton University Press.

Merton, P.A., 1953. 'Speculations on the servo-control of movement'. In: G.E.W. Wolstenholme (ed.), CIBA Foundation Symposium: The spinal cord. London: Churchill. pp. 247–255.

Miller, S., and P.D. Scott, 1977. The spinal locomotor generator. Experimental Brain Research 30, 387–403.

Mitchell, S.J., R.T. Richardson, F.H. Baker and M.R. DeLong, 1987. The primate globus pallidus: neuronal activity related to direction of movement. Experimental Brain Research 68, 491–505.

Moore, S.P. and R.G. Marteniuk, 1986. Kinematic and electromyographic changes that occur as a function of learning a time-constrained aiming task. Journal of Motor Behavior 18, 397–426.

Nagasaki, H., 1989. Asymmetric velocity and acceleration profiles of human arm movements. Experimental Brain Research 74, 319–326.

Neafsey, E.J., C.D. Hull and N.A. Buchwald, 1978. Preparation for movement in the cat, II. Unit activity in the basal ganglia and thalamus. Electroencephalography and Clinical Neurophysiology 44, 714–723.

Nelson, W.L., 1983. Physical principles for economies of skilled movements. Biological Cybernetics 46, 135–147.

Nemire, K. and B. Bridgeman, 1987. Oculomotor and skeletal motor systems share one map of visual space. Vision Research 27, 393–400.

Ostry, D.J., J.D. Cooke and K.G. Munhall, 1987. Velocity curves of human arm and speech movements. Experimental Brain Research 68, 37–46.

Partridge, L.D. and L.A. Benton, 1981. 'Muscle, the motor'. In: Handbook of physiology: The nervous system II. Bethesda, MD: American Physiological Society. pp. 43–106.

Passingham, R.E., 1987. 'From where does the motor cortex get its instructions?' In: S.P. Wise (ed.), Higher brain functions. New York: Wiley. pp. 67–97.

Piaget, J., 1963. The origins of intelligence in children. New York: Norton.

Piaget, J., 1985. The equilibration of cognitive structures. Chicago, IL: University of Chicago Press.

Pompeiano, O., 1984. 'Recurrent inhibition'. In: R.A. Davidoff (ed.), Handbook of the spinal cord, Vols. 2 and 3. Anatomy and physiology. New York: Marcel Dekker.

Pompeiano, O. and P. Wand, 1976. The relative sensitivity of Renshaw cells to static and dynamic changes in muscle length. Progress in Brain Research 44, 199–222.

Powers, W.T., 1973. Behavior: The control of perception. Chicago, IL: Aldine.

Pratt, C.A. and L.M. Jordan, 1987. Ia inhibitory interneurons and Renshaw cells as contributors to the spinal mechanisms of fictive locomotion. Journal of Neurophysiology 57, 56–71.

Rack, P.H.M. and D.R. Westbury, 1969. The effect of length and stimulus rate on the tension in the isometric cat soleus muscle. Journal of Physiology 204, 443–460.

Rack, P.M.H., 1981. 'Limitations of somatosensory feedback in control of posture and movement'. In: V.B. Brooks (ed.), Motor control. Handbook of Physiology, Sect. 1, Vol. 2. Bethesda, MD: American Physiological Society. pp. 229–256.

Renshaw, B., 1941. Influence of discharge of motoneurons upon excitation of neighboring motoneurons. Journal of Neurophysiology 4, 167–183.

Renshaw, B., 1946. Central effects of centripetal impulses in axons of spinal ventral roots. Journal of Neurophysiology 9, 191–204.

Ritter, H.J., T.M. Martinez and K.J. Schulten, 1989. Topology conserving maps for learning visuo-motor-coordination. Neural Networks 2, 159–168.

Ryall, R.W., 1970. Renshaw cell mediated inhibition of Renshaw cells: Patterns of excitation and inhibition from impulses in motor axon collaterals. Journal of Neurophysiology 33, 257–270.

Schwartz, A.B., R.E. Kettner and A.P. Georgopoulos, 1988. Primate motor cortex and free arm movements to visual targets in three-dimensional space. I. Relations between single cell discharge and direction of movement. Journal of Neuroscience 8, 2913–2927.

Shepherd, G.M., 1979. The synaptic organization of the brain. New York: Oxford.

Sherrington, C.S., 1906. The integrative action of the nervous system. New Haven, CT: Yale University Press.

Simon, H.A., 1969. The sciences of the artificial. Cambridge, MA: MIT Press.

Soechting, J.F. and M. Flanders, 1989. Errors in pointing are due to approximations in sensorimotor transformations. Journal of Neurophysiology 62, 595–608.

Sparks, D.L. and M.F. Jay, 1986. 'The functional organization of the primate superior colliculus: A motor perspective'. In: H.-J. Freund, U. Büttner, B. Cohen and J. Noth (eds.), The oculomotor and skeletal-motor systems. Amsterdam: Elsevier. pp.235–241.

Thelen, E. and D.M. Fisher, 1983. The organization of spontaneous leg movements in newborn infants. Journal of Motor Behavior 15, 353–377.

Van Buren, J.M., C.L. Li and G.A. Ojemann, 1966. The fronto-striatal arrest response in man. Electroencephalography and Clinical Neurophysiology 21, 114–130.

Viallet, F., E. Trouche, D. Beaubaton, A. Nieoullon and E. Legallet, 1983. Motor impairment after unilateral electrolytic lesions of the Substantia Nigra in baboons: Behavioral data with quantitative and kinematic analysis of a pointing movement. Brain Research 279, 193–206.

Wand, P. and O. Pompeiano, 1979. Contribution of different size motoneurons to Renshaw cell discharge during stretch vibration reflexes. Progress in Brain Research 50, 45–60.

Woodworth, R.S., 1899. The accuracy of voluntary movement. Psychological Review 3, 1–114.

Wurtz, R.H. and O. Hikosaka, 1986. 'Role of the basal ganglia in the initiation of saccadic eye movements'. In: H.-J. Freund, U. Büttner, B. Cohen and J. Noth (eds.), Progress in brain research, Vol. 64. Amsterdam: Elsevier. pp. 175–190.

Zelaznik, H.N., R.A. Schmidt and C.C.A.M. Gielen, 1986. Kinematic properties of rapid aimed hand movements. Journal of Motor Behavior 18, 353–372.